RF ENERGY HARVESTING

Submitted in Partial Fulfillment of the Requirements for the

Degree of

Bachelor of Science in Electrical Engineering Technology (BS-EET)

University of Cincinnati, Spring 2012

By Kenneth Brown, Jason Reese, and Jian Zhen

Department Advisor:

James O. Everly
Associate Professor of Electrical and Computer Engineering Technology

Table of Contents Page

List of Figures

List of Tables

1. INTRODUCTION

1.1. Background

RF energy harvesting is an idea whose time has come. Victor Hugo once remarked: “You can resist an invading army; but you cannot resist an idea whose time has come.” Today there are over 5 billion cell-phones (there are 7 billion people), 44,000 radio stations, thousands of TV stations, and countless home Wi-Fi system irradiating RF energy into the atmosphere. Before 1885 when Marconi made his first radio, anthropogenic RF did not exist in our environment. All anthropogenic RF energy is generated from electrical energy what in turn is generated by fossil fuels that in turn produces CO2 resulting historical global warming. This is a proof of concept project to show that ambient RF can be harvested, stored, and reused. Figure 1 is a 2002 map of commonly known radio towers in the United States by Meuser plotting 20,455 cell; 39,730 pagers; 241,258 microwave; 1,714 television; 4,789 AM; 6,014 FM; and 589,300 private tower locations.

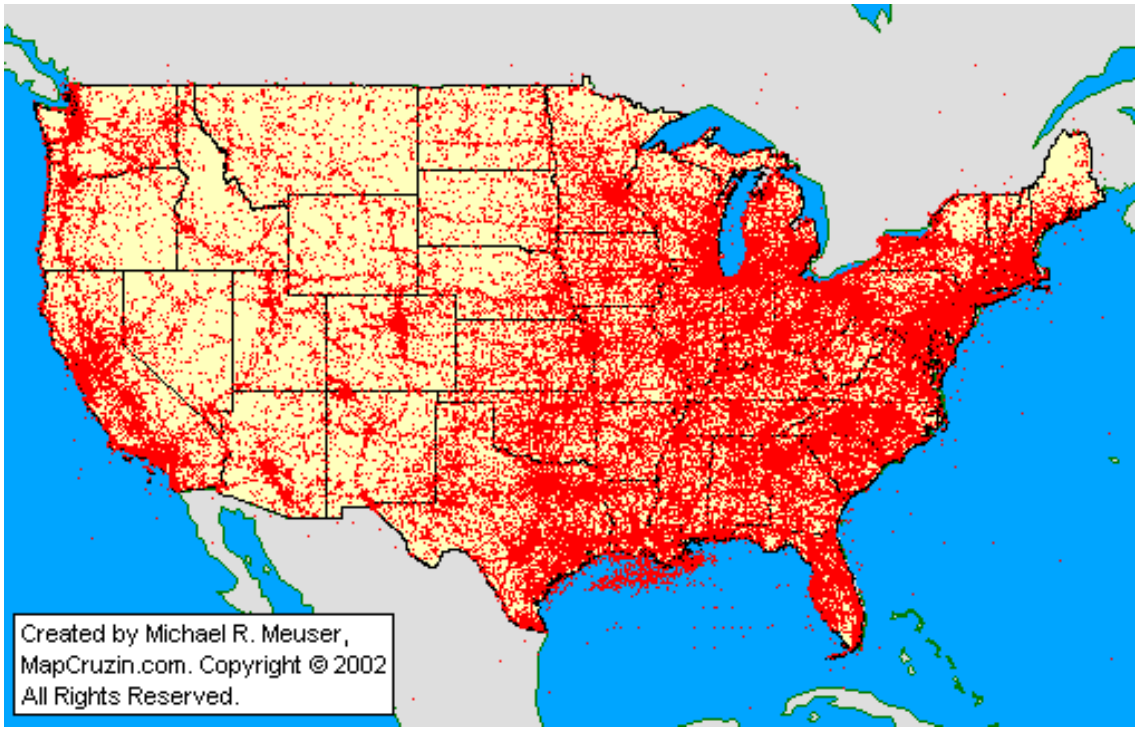

Figure 1. Meuser's mapping of radio towers in the US, potential sources of RF energy.

This project addresses needs felt across many sectors of industry. As the demand for energy increases, the need for energy efficiency grows in stride. Modern microcontrollers can operate on less than 200 micro-amps of current, and this is already considered “ultra low” current. Despite the already “ultra low” label, the bar continues to be lowered every year. How low power consumption can go will be determined by future hands, but the power supply that can run these super-ultra-low consumption devices is already at our fingertips.

We are aware that harvestable ambient RF energy is a full order of magnitude below what can be harvested from ambient wind and solar sources. However, this does not remove the need

for RF harvesting research and development efforts because solar and wind energy have various physical and time limitations. RF energy, on the other hand, is pervasive and nearly unstoppable. Behind walls, in still or windy air, in sunshine or dark, underground or underwater, RF energy is capable and available.

This is a proof of concept project to demonstrate that RF energy between from the AM radio band region of the spectrum can be collected by an antenna, rectified and multiplied by a Villard voltage multiplier, stored in a super capacitor, and used to power an microprocessor application. This report describes the antenna, the Villard voltage multiplier, the super capacitor, and a low power embedded microprocessor application used to for this feasibility demonstration.

1.2. Technical Background

The amount of RF energy available to harvest from a radio tower, power density Pd, is dependent upon the power being emitted P from the RF source, the gain - directionality of the antenna G, and the distance from the antenna r from the transmitter, as shown in equation 1.

$$P_d = PG/(4\pi r^2)$$

The Power density at the University of Cincinnati campus was calculated for 10 AM radio stations, 36 FM stations, and 22 TV stations found within 50 km of the campus. In addition, the power density was calculated from 780 cell towers within 4.8 km. Each station's geographic coordinates and transmitting power was obtained from FCC databases [1],[2], and [3]. The results were sorted and the top 33 stations were plotted in Table 1.

Table 1. Top 30 strongest radio stations near UC campus

RF source	Type	kW Pw	Km to OCAS	µW/cm2 at OCAS	MHz
WCPO-TV	TV	880	1.25	45	519
WLWT	TV	1000	3.18	8	597
WBQC-LP	TV	150	1.25	8	501
WOTH-CA	TV	140	1.25	7	615
WCET	TV	400	3.18	3	591
WPKF556	CELL	0.5	0.13	2	463
WBQC-LP	TV	39.7	1.25	2	537
WNLC568	CELL	0.5	0.14	2	463
WNVN408	CELL	0.5	0.14	2	463
KNKL832	CELL	0.5	0.14	2	931
KNNU922	CELL	0.5	0.18	1	462
KNBL786	CELL	0.5	0.18	1	462
WSA736	CELL	0.5	0.18	1	461
WSS280	CELL	0.5	0.18	1	461
KNAD373	CELL	0.5	0.18	1	461
WPMX504	CELL	0.5	0.18	1	452
KKY370	CELL	0.5	0.18	1	462

KNBU559	CELL	0.5	0.18	1	461
WVXU	FM	26	1.29	1	92
WPTO	TV	400	5.42	1	555
WNSY613	CELL	0.5	0.19	1	308
WNVD938	CELL	0.5	0.19	1	158
WPYE541	CELL	0.5	0.19	1	152
WPMV941	CELL	0.5	0.19	1	929
KQD599	CELL	0.5	0.19	1	152
WPYM345	CELL	0.5	0.19	1	152
WGUC	FM	18.5	1.26	0.9	91
WOTH-LD	TV	15	1.25	0.8	507
WBQC-LD	TV	15	1.25	0.8	669
WUBE-FM	FM	14.5	1.26	0.7	105
WXIX-TV	TV	227	5.42	0.6	561
WOFX-FM	FM	16	1.58	0.5	93
WNNF	FM	16	1.58	0.5	94

While it appears that TV stations would have provided the strongest source of RF for this project coming from megawatt transmitting towers, AM stations were chosen because we did not have access to VHF simulation software or instrumentations. So the project considered an AM stations as a source of ambient RF, 0.35 µW/cm2 from WDBZ one km away (not the top 30 Table I), in order to work in HF region. We also conducted field studies 3 miles for a 50 kW station, WLW, 700 kHz.

The law of conservation of energy, first formulated in the nineteenth century, is a law of physics. It states that the total amount of energy in an isolated system remains constant over time. Thus, energy is neither created nor destroyed but changes form. RF is just one form of energy. Most RF energy is generated from electrical energy that in turn is generated from fossil fuel chemical energy. These fossil fuels are limited natural resources. Most RF energy is wasted in that it is either released into outer space or absorbed into the environment and converted to heat. Only a small percentage of RF reaches its intended purpose. This project proves the concept that RF energy can be captured, converted to electrical energy, stored, and reused

2. SOLUTION-METHOD

2.1.The Antenna

2.1.1. A heuristic introduction

Considering maximum effective aperture as the desired setpoint for our antenna selection, the ideal candidate antenna for the medium wave AM broadcast band would

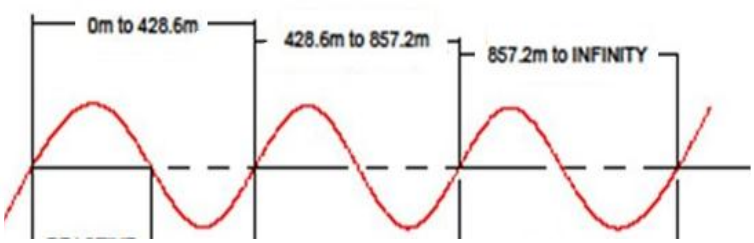

Figure 2: 3 Wavelengths at 700KHz

have been without a doubt the longwave antenna. The longwave antenna, as its name indicates, is called a "longwave" antenna because the wire defining its dimensions unwinds into a full wavelength. This would not be a problem at higher frequencies like 2.4 GHz where the wavelength is a scant .125 meters, but at medium frequencies like 500KHz, 700KHz, or 900KHz, it is not a simple task. A true longwave antenna for a radiated electromagnetic wave varying in time at 700,000 cycles per second, for example, would need to be approximately 430 meters long. This certainly would give us a large physical aperture, and coupled with even mediocre aperture efficiency, would easily give us the highest effective aperture for our desired medium frequency bandwidth.

The parameters of this project defined a transducer (an antenna is a transducer since it converts time varying electric currents to and from radiated electromagnetic waves) that operated at 700,000Hz, was mobile enough to transport between the lab and field, affordable within the confines of a senior design project, and provided the best effective antenna aperture. Electrical aperture (W/m^2) is the amount of power that can be captured from the power density of a plane wave, and delivered to a load between the antenna's terminals. The longwave antenna was a clear winner in the antenna aperture department, but considering we were not even 100% certain that our RF Harvesting approach was valid, a 430 meter antenna was clearly not within our limitations. Despite our desire to have the greatest effective antenna aperture imaginable, the space and cost implications of the longwave antenna lead us to our next best transducer option, the spiral wound air loop antenna.

Cost, size, and immobility are some of the major disadvantages of a true longwave antenna. The spiral loop antenna, though sizeable in its own right, does not need to be a full wavelength long. The spiral loop air core antenna can operate as a relatively high aperture antenna at approximately 1/10th of a wavelength or less. This instantly reduced the proposed footprint of our project to $1/10^{th}$ the size of the longwave antenna, and also provided us a situation where we could test our project in the lab as well as the field. Although the construction still called for more than 40 meters of wire, the spiral shape made the antenna compact enough for our needs. The loop antenna could have been constructed using an edge wound design. Whereas the loops on a spiral wound antenna get progressively smaller, the loops of an edgewise antenna are all the same size. The major advantage of the edge wound antenna would have been the fact that most of the equations available are built around this type of antenna. These equations are at best only approximations of reality, but they are still very helpful to have during the design process. The UMR-EMC Lab Formula is an example of this. We tried to port the desire parameters of the spiral wound antenna into the confines of the UMR-EMC formula, but did not get dependable results. In retrospect, the availability of these types of equations should have tipped the balance in favor of an edge wound antenna. Thus is the power of retrospect.

The spiral loop antenna is considered a highly directional antenna. This high directivity means that the antenna reception is much more focused than an isotropic antenna. An example of a low directivity antenna would be a cell phone antenna because a signal from any direction can be received. The spiral loop does not work like this, and must be positioned carefully to take advantage of the antenna's areas of maximum gain. For the spiral wound antenna, the signals received at the antenna's sides are received, while signals coming in off the sides are greatly

attenuated. I will attempt to explain this better later, but for now knowledge that the spiral antenna has high directivity will suffice. The longwire antenna is also a high directivity antenna, but the compact size of the spiral loop allows for it to be repositioned easily to manipulate the nodes and nulls. With this in mind, early in the design process we knew that the antenna would need to be mounted to a stand that had full alt azimuth rotational ability in order to maximize its figure 8 reception pattern.

One of the main advantages of the spiral loop antenna (using the longwave antenna as our reference frame) is that it can comfortably fit inside the trunk of a normal sized car. Our primary goal was to prove the concept of RF Harvesting, so we knew that we would be required to spend many hours tied to the University laboratory room operating under controlled conditions. We could not deny, no matter how hard we tried, that we wanted to get the harvester working in the field. From day one of the project it was clear to us that we wanted to design our antenna so that we could perform field tests. The ability to transport the antenna from the lab to field, from the lab to each of our homes, enabled the prospect of field testing. This was made feasible by the spiral loop antenna.

2.1.2. Early calculations

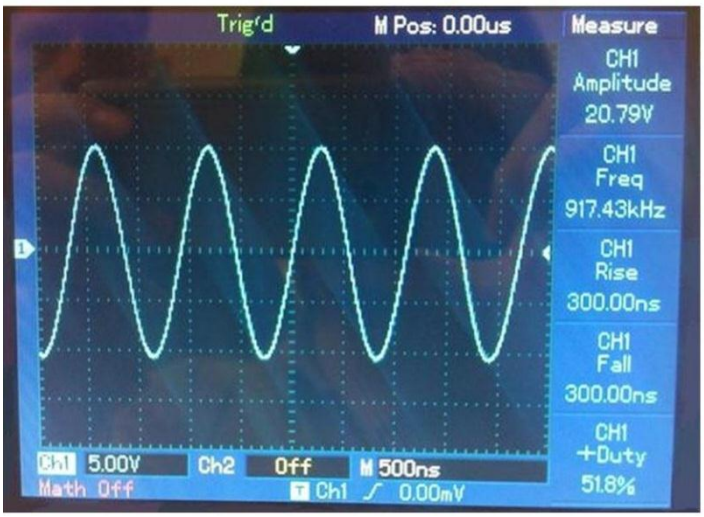

Figure 3: 10 Volt Peaks we Observed at our

The designer of the antenna must determine the size of the loop. The amount of gain you can get from a loop antenna is dependent on the size of the loop. A larger area translates into larger (directional) gain. At over 40 meters, our spiral antenna design would still be considered a small loop antenna because it is less than 1/10th of a wavelength. Smaller loops can be built but most certainly would require an amplifier at the antenna terminals in order to be effective. An amplifier would have nulled the purpose of harvesting RF energy, so all of the smallest loop options were removed from the table. An equation that we used early in the design process, $V_o = \frac{2\pi ANE_f Q cos(\alpha)}{\lambda}$, relates the effect of the antenna's area to the voltage produced at the terminals of the antenna. This equation was intended for an edge wound air loop antenna, but it is still effective for explaining the principles involved with a spiral wound loop. *A* is the area of the loop, *N* is the number of turns of wire in the loop, E_f is the strength of the signal in volts per meter (V/m), α is the angle of arrival of the signal, Q is the loaded Q of the antenna when the air capacitor is added to the circuit, and λ is, of course, the wavelength of the electromagnetic wave. Since area is in the numerator of this equation, we wanted to get it as close to 1m as possible (of course 2,3,or 4 meters would have been better but would have reduced the portability factor). However, increasing the area of the loop has a tradeoff in the numerator. *N*, the number of

turns, is reduced as the area of loop expands. We estimated that a 1 meter loop would require approximately 20 loops of wire. An electric field strength of 2V/m, with an antenna Q of 90, and an angle of 0° to the transmitting antenna would give us approximately 50 volts at the output of our loop. Knowing that this was at best an approximation of reality, we were still encouraged by the calculations. Theoretically we could build an antenna at 700KHz that would produce more than enough voltage at its output terminals to charge a supercapacitor to a working voltage.

2.1.3. Construction of receiving antenna

The spiral loop air core antenna (again using the longwave antenna as our reference frame) can be relatively easily and cheaply constructed for medium frequency applications. The tools list was modest and consisted of a drill, a saw, approximately 50 meters of 18 to 24 gauge wire (AWS), some wood glue, and an alt azimuth capable stand. We wanted to make a quick and dirty prototype of our antenna. The short materials list was a definite plus since the addition of the prototype would cause us to construct the antenna at least 2 times.

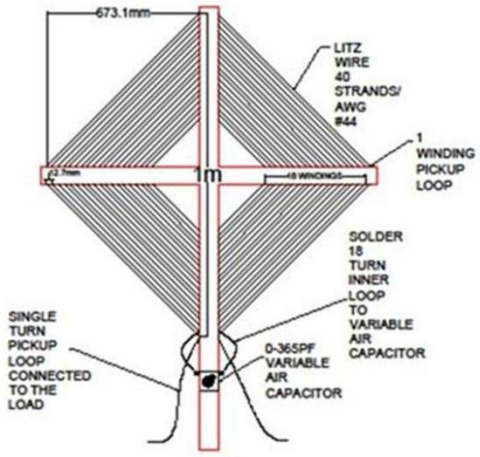

Figure 4 Antenna schematic.

The first spiral loop antenna we built was made with 18 gauge stranded bare copper wire. Early research revealed that performance did not depend on whether the antenna was wound with single strand or multiple strand wire, insulated or bare, 18 gauge or 22 gauge. We felt strongly that any combination of these characteristics would not have a noticeable impact on the effective aperture of our antenna.

Researching one characteristic of the wire did reveal a performance dependent material component. The only copper wire that we found to be readily available was stranded copper wire. We knew that stranded wire would not affect our design, but we thought a single strand of wire would be easier to work with, as well as make our overall design look better. We considered replacing the stranded copper wire with single stranded aluminum wire. Our local hardware store carried the length of single stranded bare wire that we desired, but in aluminum and not copper. Our early research indicated that this would not be a problem, but as we dug deeper into this question we uncovered claims and data that indicated substituting aluminum wire would cost our antenna nearly 3dB of signal strength. This was clearly not acceptable for our transducer, so we decided to use the stranded bare *copper* wire since it was readily available in the 43 meter lengths we required. Our later research would lead us to an altogether different type of wire to use for our final presentation antenna, Litz wire. I will discuss Litz wire later. At this early stage, it is important to note, we were completely unaware that Litz wire even existed.

The choice of frame material came down to wood versus PVC pipe. To be honest, the PVC pipe would have probably been the best choice because it is a light, cheap, and sturdy material. PVC pipe would have given us more flexibility for design changes, and would have been more rugged overall. However, we had plenty of free wood available to us that was also light, sturdy, and rugged enough. We had a specific design in mind, and since free costs less than cheap, we decided use the free wood for our frame.

With our antenna material in hand, it was time to actually construct the prototype antenna. We cut one piece of wood slightly larger than a meter, and then cut another two pieces of wood slightly larger than half a meter apiece. We drilled 40 holes into our meter length wood, and then drilled 20 holes into each half meter length. In all we drilled 80 holes into our frame with a hand power drill. The hand drill produced somewhat crooked holes through our wood, so we decided that for the presentation antenna it would be essential to use a drill press. Regardless, the crooked prototype holes would eventually contain 19 loops of multi-stranded 18 gauge copper wire that we hoped would respond effectively to the magnetic component of the radio wave.

The antenna schematic dictated that the wire was to be wound in a square pattern that spiraled inwards at approximately 25mm's per loop, and included a separate external loop known as a pickup coil. The idea was to have the inner loop connect directly to the variable air capacitor, and the then the pickup loop would connect directly to the input of our voltage multiplier. The pickup loop is essentially a secondary winding that helps impedance match, and therefore transfer, the captured signal to the intended load. In total, counting the inner loop and the pickup coil, the amount of wire used for our prototype antenna was a little bit less than the size of 1/10th of a wavelength of a radiated electromagnetic wave varying in time at 700,000 cycles per second, which is approximately 43 meters of wire.

I do not want to conclude the antenna construction section without first mentioning the difficulties we faced while weaving the wire around the antenna frame. Although not a complete comedy of errors, wiring the prototype antenna was certainly made more difficult because of the stranded copper wire. We thought the logistics to snake 43 meters of stranded wire around 1 meter spiral loop was daunting enough. To make matters worse, If we weaved the stranded copper wire too fast, the wire would kink so we would have to stop the process and fix the kink. When a kink formed, the copper fibers began to separate. This forced us to carefully, and slowly, pull the wire through nearly 80 separate holes.

Another problem with the stranded wire was that pulling at a pace slightly above "slow" would cause the stranded wire to splinter apart at its end. When this splintering occurred, we would have to stop and attempt to tighten the strands of wire. However, the wire would never regain its original compactness after it became splintered, making it harder to feed the holes. We thought that if we pulled the entire length of wire, all 43 meters of it through each individual hole, then the kinking and splintering would abate. The problem with pulling the full length of wire individually through each hole, though it would have been the easiest method, was that we had no good place to store the 43 meters of wire each time it was pulled. If we let the wire pile up into a mound, it would tangle up like a string of Christmas lights in a storage box!

Probably the best place to construct this spiral loop antenna would have been at a football field!

In the end, to prevent tangling of the wire, we had to lay the wire all over the lab as we pulled it through each hole. We wrapped the stranded copper wire around chairs, tables, and backpacks, all in an effort to prevent the wires from tangling into an unworkable mass. As if to compromise with the physics and mechanics of the wire, we chose to manually pull a few meters at a time in an attempt to eliminate the negative effects inflicted on the structure of the wire.

After much perseverance, the prototype antenna was finally complete. Feeling that every good prototype needs a name, we decided to call our initial prototype antenna the *Silver Surfer*. We did not have our Ramsey 100mW rated transmitter working at this point in time, so we were unable to test our prototype in a controlled laboratory. For this reason, after first attaching a near-zero to 365pF variable air capacitor to the inner coil of the spiral loop antenna, and then attaching the pickup coil of the *Silver Surfer to* an oscilloscope, we went directly to the field to see if we could actually catch any radiated electromagnetic waves.

2.1.4. Field testing with electrolytic capacitors

Our primary frequency of interest was 700,000 Hz. This being our goal, we chose Mason, Ohio as our primary field test site. We knew that the closer we could get to a powerful source of transmission, the greater the chances became to obtain a harvestable magnitude signal. With this in mind, we chose Mason.

Mason, Ohio is home to a major transmitting antenna for 700WLW. No longer the source of RF energy for Mr. Powell Crosley's 500,000W monolith, Mason is still the home of powerful 50,000W transmitter. With the oscilloscope connected in parallel with the variable air capacitor, we observed a maximum of approximately 10V peaks with our antenna at the Mason test site. We estimated that we were over 4 kilometers from the 50 kW transmitter, meaning we were clearly in the far field of the transmitting antenna. Being in the far field of the radiating antenna was an essential component of our field studies, since in the lab near-field harvesting was unavoidable at 700KHz.

After verifying the voltage across our capacitor, the antenna was connected a prototype 10-stage voltage multiplier to the prototype antenna. Applying the test voltage multiplier in parallel with the antenna reduced the amount of Voltage obtained across the air capacitor to just a volt or two. Despite this, the voltage multiplier rectified the radiated electromagnetic signal, and multiply it into approximately 10 Volts DC at the final stage of the multiplier. Now the only procedure that remained was to test whether or not the harvest could be captured, rectified, and multiplied energy into a capacitor.

We used a standard electrolytic capacitor for our initial field tests. We felt that the lower RC time constant was more apt to provide observable results. The result of this, though not earth shattering to the RF harvesting initiated, was profound to us. We were able to harvest RF energy into the electrolytic capacitors. There was enough energy density between the output ports of the voltage multiplier to couple with the low RC time constant of the electrolytic

capacitor to store an electrical charge smoothly and fast. The charge time was minimal as we expected. We were encouraged by these early results from the electrolytic capacitors. We were certain now that anthropogenic RF energy could be captured, stored, and utilized. Moreover, we knew that our antenna was an effective transducer for the electromagnetic waves, and would supply a voltage multiplier with a working electrical charge! Ma

2.1.5. Harvesting into supercapacitors: ESR's effect on antenna q factor

Harvesting into electrolytic capacitors was a milestone for the project. However, electrolytic capacitors do not offer enough energy density to run our Texas Instruments application. Super capacitors do provide an adequate energy density, but impose a different set of conditions into our harvesting circuit. The early results proved to us that our spiral loop could at least operable with the concept of harvesting ambient RF energy, but whether or not it would interface well with a supercapacitor was still a question. The spiral loop antenna would have to work with a supercapacitor in order to prove that RF harvesting can be utilized to supply a low power data recording application.

As the equation $V_o = \frac{2\Omega ANE_f Q cos(\alpha)}{\lambda}$ dictated, we were concerned about the effect of adding a super capacitor and voltage multiplier to the antenna's circuit in respect to the Quality factor (Q factor) of the antenna. The Q factor characterizes an antenna's bandwidth relative to its center frequency. A higher Q factor means that the antenna has a lower rate of energy loss relative to the energy it can store $\left(\frac{ENERGY\ STORED}{POWER\ DISSIPATED}\right)$. Basically the Q factor indicates the rate at which the oscillations die out after they have been initiated. To understand Q factor, it is helpful to consider a bell analogy. A typical bell is a high Q factor element. When the underdamped Bell is struck, it oscillates for a long period of time. Imagine that the bell was filled with concrete. A bell filled with concrete will not resonate at all when it is struck, and is representative of overdamped antenna with a low Q factor. Obviously, we want our antenna to resonate at the highest amplitudes possible when struck with an electromagnetic wave. We understood that a higher Q factor means that the antenna would resonate around a much smaller bandwidth of frequencies, but we felt the tradeoff justified the pursuit of a high Q factor. It is important to note that capacitors and antenna's both are considered to have Q factors based on the ratio of $\frac{ENERGY\ STORED}{POWER\ DISSIPATED}$.

When considered as a lumped element model, the capacitor is actually a resistance in series with a capacitance. The lumped element model reveals what is known as the Equivalent Series Resistance (ESR), and represents the fact that a capacitor is not an *ideal* element. An ideal capacitor would not dissipate any energy. A real capacitor does dissipate small amounts of energy and this non-ideal behavior is characterized by ESR. Super capacitors have an ESR of approximately 50Ω, while electrolytic capacitors have an ESR of 3Ω's or less.

The affect of ESR, and resistance in general, on the Q factor of the antenna was a concern for us as we designed our harvesting circuit. Our harvester circuit be represented as a single circuit containing resistance, inductance, and capacitance (RLC circuit). For a series RLC circuit, the Q factor can be calculated as $Q = \frac{1}{R} * \sqrt{\frac{L}{C}}$. This formula indicates that a higher resistance would

mean a lower Q for a series RLC circuit. The RLC circuit we were considering, however, was a parallel circuit. The Q factor for a parallel RLC circuit is defined as Q =R* $\sqrt{\frac{C}{L}}$. This means that a smaller resistance in parallel with the resistance of the circuit would reduce the Q factor of the antenna, and that a higher resistance was desirable for our circuit.

Ideally we wanted an infinite resistance between the output terminals of our spiral loop antenna, in parallel with the variable air capacitor. This would preserve the bandwidth of our antenna and ensure that it would resonate at the highest amplitudes possible when struck by our specific electromagnetic wave. An ESR of 50Ω for the supercapacitor is not an infinite resistance. On the other hand, neither is the 3Ω resistance for the Electrolytic and it charged up without a problem. For the supercapacitor, antenna Q factor was more of a consideration because we were no longer dealing with microfarads in our RC time constant, but we had .33 farads to consider. The greatly reduced RC time constant for the electrolytic capacitor could endure an overdamped antenna, whereas for the supercapacitor charge curve it could not be ignored. We needed to resonate at the highest amplitudes possible in order to charge the supercapacitor at a rate that would sustain a real world sensor application.

2.1.6. Voltage multiplier and the antenna

I do not want to attempt to characterize the voltage multiplier circuit in this section. My main goal of this section is to describe the thought process we underwent when considering the affect of the voltage multiplier on the antenna circuit. I will also present some of our observations. To see a more detailed characterization of the voltage multiplier, the voltage multiplier section of this report should be consulted.

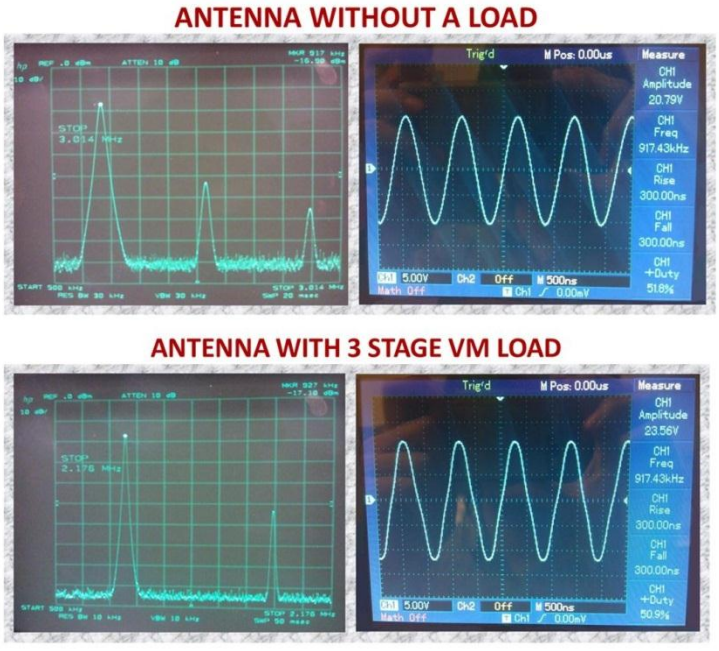

Figure 5. Spectrum analyzer screenshots with and without

From an antenna standpoint, the considerations for the Voltage Multiplier were the same as the considerations for the Supercapacitor. Would introducing the voltage multiplier overdamp or underdamp our resonator? Considering the Q factor for our parallel RLC harvester circuit was still Q =R* $\sqrt{\frac{C}{L}}$, the coup de grace to the resonance of our antenna would be a small parallel resistance. We already had the low ESR of the supercapacitor to consider, we did not want to compound the problem by designing a minimal resistance voltage

multiplier. Our intuition told us that more multiplier stages in parallel would mean a lower overall resistance. Our testing reinforced this claim. The amplitudes we were able to resonate at were greatly attenuated by the higher stage voltage multiplier. If we could resonate at 10 volts using only the variable air capacitor, the amplitudes would be reduced to less than one when the 10 stage multiplier was introduced into the circuit. If this was the case, and our thinking on the matter was correct, a lower stage multiplier would reduce the amplitude of our signal by much less. This is indeed what we observed. When a 3 stage voltage multiplier was interfaced with our spiral loop antenna, the voltage amplitudes actually increased!

2.1.7. Towards the goal of harvesting RF energy

With a better understanding of the overall design decisions we had to consider, and in possession of a positive electrolytic capacitor RF energy harvesting experience, we embarked upon the ultimate goal of harvesting RF energy into Electric Double Layer Capacitors (aka Supercapacitors). Whereas we were able to charge the electrolytic capacitors in just a few seconds, the supercapacitors would initially take several days to charge. The energy density, and the RC time constant to reach this energy density, is much lower for electrolytic capacitors than for supercapacitors, and therefore it takes more time to charge them to full energy capacity. This and the Equivalent Series Resistance differences between Electrolytic and Electric Double Layer Capacitor were the main charge time culprits. Regardless, we knew that our concept had been proven. We knew that our approach was effective, and that our antenna and voltage multiplier designs worked. Our main concern moving forward was charging the supercapacitor in a reasonable amount of time. Though charging a supercapacitor in a few days certainly proves our concept, it does not provide enough energy to power or RF transmitter application. How could RF harvesting be considered a useful technology if we could not even run one of the worlds most low power microcontrollers with it! We were positive that if we made alterations to our design we would be able to harvest at a faster rate. Could we actually run a real world application with RF harvested energy? That was still to be determined.

Figure 6. RF energy Harvesting

2.1.8. Design improvements and triumph

We decided to build a better spiral loop antenna. The *Silver Surfer* was effective but aesthetically a mess. The strands of wire that had become separated during the initial winding were made worse by field tests. The copper colored paint job we chose for the wooden

structure was only semi successful, and the overall dimensions of the antenna were not precise. We decided to abandon the stranded copper wire (which was not a hard decision to make) in favor of some relatively more sophisticated "Litz" wire. Litz wire consists of many tiny individually insulated wires. The purpose of Litz wire is to reduce the increased AC resistance (aka the *Skin Effect*) the wire experiences when an alternating current is applied to it. This improvement should reduce the power loss of the antenna and increase the antenna's Q factor. We also wanted to increase the area of our loop while maintaining the highest number of loops possible. Our goals here were to maximize the voltage available to us at our output terminals according to the equation $V_o = \frac{2\Omega ANE_f Q cos(\alpha)}{\lambda}$. Aesthetically, we wanted to use a drill press instead of a hand drill in order to improve the precision of our holes. The paint job was abandoned as well, in favor of the natural tan color of the boards that comprised the antenna structure.

The new antenna was an instant improvement. The better dimensioning and Litz wire were definitely driving factors toward better reception ability. Each loop was more evenly spaced at approximately 25.4mm, and the furthest dimension of the outer loop drill holes were exactly 1 meter. The Litz wire introduced some major soldering problems for us, because the insulation on each strand of wire had to be removed before soldering. We achieved good conductivity with our solder by utilizing the cross area created from cutting the wire into separate pieces. The cross area for each strand of wire did not have any insulation because the insulation only covered the circumference of the wire. We soldered the cross sectional area parallel to small copper "islands", and from these copper islands we were able to attach our variable capacitor and meter probes to the antenna Litz wire. The Litz wire made weaving the 43 meters of wire to the frame relatively simpler as well. The Litz wire, and the firmer and better dimensioned construction, nearly doubled our lab reception voltage.

Concurrently with building the new antenna, we were able to employ a 100mw transmitter at the senior design test lab. No longer RF attenuated by the brick College of Applied Science walls, we were able to harvest energy at our convenience with our antenna, voltage multiplier, and supercapacitor. Although still slow, the charge times were improving. We were able to power a Texas Instruments MSP430 with a supercapacitor and send temperature information over a USB cable to a GUI that we designed. This displayed for us the capability of a super capacitor to supply energy to an embedded device. We wanted to improve upon the wired connection to the GUI, so we decided that we would transmit the data remotely to a GUI using a Texas instruments transceiver. We wanted our harvester to completely sustain the energy required to transmit its voltage and temperature information. This breakthrough came when we properly grounded the transmitting antenna from the Ramsey. With this we were able to sustain the supercapacitor charge enough to perpetually sustain the energy requirements for wireless transmitter application. More work is needed to improve harvesting a far field RF signal. We were able to harvest a far field signal, but not at the rates attained in the near field. In the near field at least, the spiral loop antenna helped us achieve the goal of an RF energy supplied wireless transmitting device.

2.1.9. Directivity of reception pattern better explained

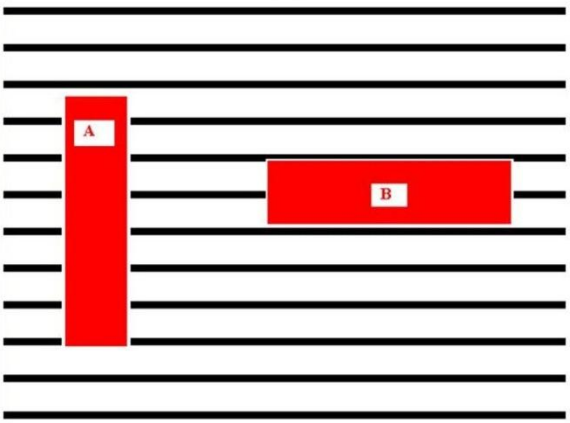

Figure 7. Advancing radio wave

As mentioned earlier, the spiral loop antenna is a high directivity antenna, and does not receive the same magnitude of signal in every direction. This means that the gain of the antenna is maximized at particular nodes along the geometry of the antenna relative to an isotropic antenna, which receives a signal equally from all directions. High directivity also means that there exist nulls relative to the geometry of the antenna where there the antenna gain is low.

For a signal to be received by an antenna, a potential difference in voltage must exist across the wire in order to induce a current through the wire. The geometry of the antenna where this effect is maximized is called a node of the antenna. Imagine that each red rectangle above is a birds eye view of a single loop of wire on our antenna. Also imagine that every black horizontal line represents an isopotential line where the voltage is the same. For red rectangle A, it is easy to imagine the potential voltage difference across the length of wire. For red rectangle B, on the other hand, the potential difference is much less. When the spiral loop antenna is positioned like Red rectangle A above, there exists a Node where the gain relative to the gain of an isotropic antenna is the highest. When the spiral loop antenna is oriented like Red rectangle B, a Null appears where the gain relative to the gain of an isotropic antenna is the lowest. The angle of arrival of the RF signal is an important factor as well. Remember the equation $V_o = \frac{2\Omega ANE_f Q cos(\alpha)}{\lambda}$? It is directly working of the above principles. The angle of the arriving signal is represented by α. You can see that α is used inside of a cosine function. Imagine that Red Rectangle A represents 0° and Red Rectangle B represents 90°. You can see that when a cos(0°) is inserted to the equation, $\frac{2\Omega ANE_f Q}{\lambda}$ is multiplied by 1. However, when cos (90°) is inserted into the equation, $\frac{2\Omega ANE_f Q}{\lambda}$ is multiplied by 0!

3. RF rectification and voltage multiplier

The diode semiconductor device is paramount to RF rectification and multiplication. This passive device converts AC current to DC current, but while doing so, is non-ohmic in the effect of voltage upon current going through this device. The diode equation represents its general relationship between voltage and current. The William Bradford Shockley Jr. diode equation 1 is show below.

1. $I = I_S(e^{V_D/(nV_T)} - 1)$ where $V_T = \frac{kT}{q}$

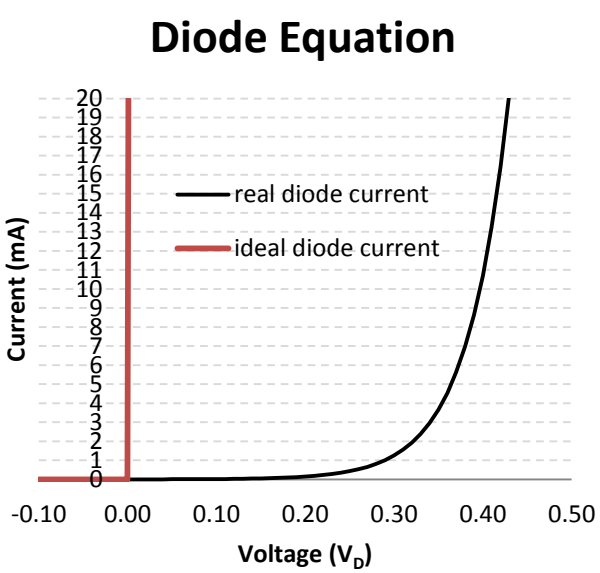

Figure 8. The Shockley diode equation and ideal diode.

I is the diode current,

I_S is the reverse bias saturation current

V_D is the voltage across the diode,

V_T is the thermal voltage, and

n is the ideality factor,

The Shockley equation and its plot in figure 2 shows the non ohmic I vs V properties that are basically exponential in shape and are influenced by the junction potential (Is) related to forward voltage, the voltage across the diode (V_D), and temperature. The non-ideality factor is a function of semiconductor material and fabrication process and adds to the forward voltage. The ideal diode would have properties as shown in figure 8, i.e. no current until the voltage reaches 0 V and then switch to infinite current. In other word, the ideal diode would act as switch on at all positive voltages. Finding a diode that approaches ideal in behavior would be best for low voltage RF signal rectification.

Modeling diode behavior in simulation software goes beyond the Shockley equation adding nuances that predicts behaviors for AC signal. This project used LTSPICE software that is free and allows for the use of third party SPICE models enabling the prediction of RF harvesting circuits. Notice that the SPICE activation energy for the Germanium and Schottky diodes are close in value meaning that both approach ideal diode behavior to about the same extent. We will not go into the extended equations used in SPICE algorithms.

Table 2 SPICE Diode Parameters next page

Table 2 SPICE Diode Parameters Used for Software Simulation				
Symbol	**Name**	**Parameter**	**Units**	**Default**
I_S	IS	Saturation current (diode equation)	A	1E-14
R_S	RS	Parsitic resistance (series resistance)	Ω	0
n	N	Emission coefficient, 1 to 2	-	1
τ_D	TT	Transit time	s	0
$C_D(0)$	CJO	Zero-bias junction capacitance	F	0
φ_0	VJ	Junction potential	V	1
m	M	Junction grading coefficient	-	0.5
-	-	0.33 for linearly graded junction	-	-
-	-	0.5 for abrupt junction	-	-
E_g	EG	Activation energy:	eV	1.11
-	-	Si: 1.11	-	-
-	-	Ge: 0.67	-	-
-	-	Schottky: 0.69	-	-
p_i	XTI	IS temperature exponent	-	3.0
-	-	pn junction: 3.0	-	-
-	-	Schottky: 2.0	-	-
k_f	KF	Flicker noise coefficient	-	0
a_f	AF	Flicker noise exponent	-	1
FC	FC	Forward bias depletion capacitance coefficient	-	0.5
BV	BV	Reverse breakdown voltage	V	∞
IBV	IBV	Reverse breakdown current	A	1E-3

LTSPICE was used to model all the circuits for this project using SPICE models found on the internet for the common diodes 1N5819, 1N4001, 1N34A, and 1N5711. LTSPICE uses a graphic interface as shown in Figure 9. The 1N4001 diode was not seriously considered as a candidate because of its classic high forward voltage of 0.6 V. However, the Schottky diodes 1N5819 and 1N5711 were compared to the 1N34A germanium diode that has been used for decades for weak signal rectification. The 1N34A was not considered because not available in SMT. The 1N5819 was considered because of its cheap surplus price of $0.33 and the 1N5711 because it was a through hole style equivalent to the HS282 SMT. This project used ugly construction prototyping for proof of concept requiring the older though hole style leads.

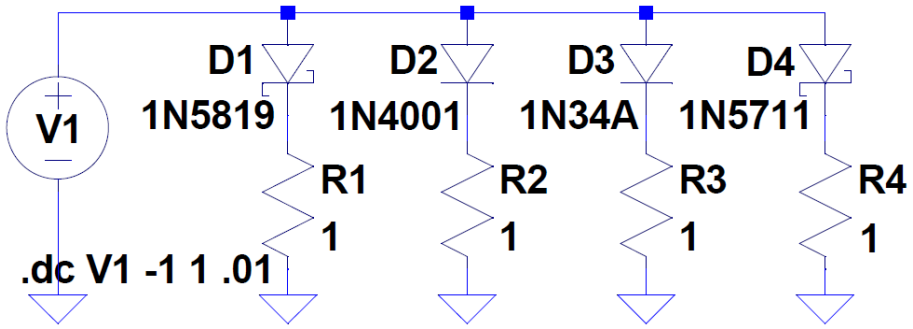

Figure 9. LTSPICE graphical circuit interface comparing diodes

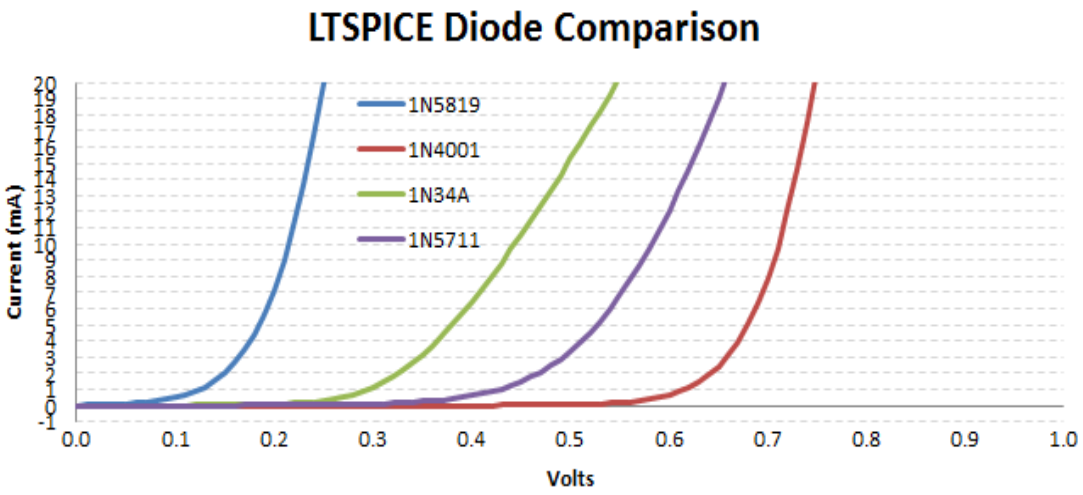

Figure 10. I-V results from LTSPICE simulation comparing diodes.

In Figure 10, the LTSPICE simulations shows which diode would most closely approach ideal I-V behavior for project development. Definitely, the 1N4001 was the farthest from ideal and not considered. This project worked with the two different types of Schottky diodes, the 1N5819 and 1N5711. Thus, the DC resistance of the diode in its active region is close to 1/slope. Figure 3

shows the 1N5819 to have the lowest resistance, about the same as the 1N4001, but also low forward voltage. However, Professor Everly showed in his presentation, “Back to the Future” [10], that it is better to look at the AC resistance of the diode. Everly equates that to equation 2. This may be a more accurate assessment of VM impedance.

2. $Z_d = V_T\eta / I_S$

Figure 11 is a circuit comparing a 1N5711 with and without a capacitor for converting RF to DC. The 1N5711 diode is a through the hole equivalent to the Agilent HS282 used by Harris in his voltage multiplier circuit. It was selected for this study [9]. This project used 100 uF tantalum capacitors. The tantalum capacitor is a second generation capacitor that distinguishes itself from older capacitors in having high capacitance per volume and weight, lower equivalent series resistance (ESR), lower leakage, and higher operating temperature than other electrolytic capacitors. Better than disc and paper capacitors, while cheaper than super capacitors, Tantalum was used for the VM effectively.

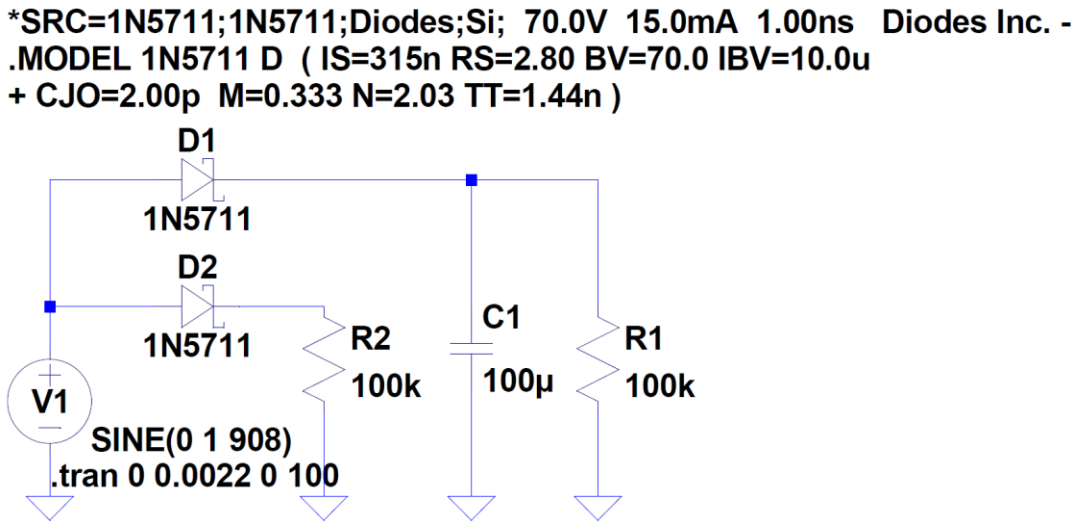

Figure 11. LTSPICE rectification of 908 kHz RF using a 1N5711 diode.

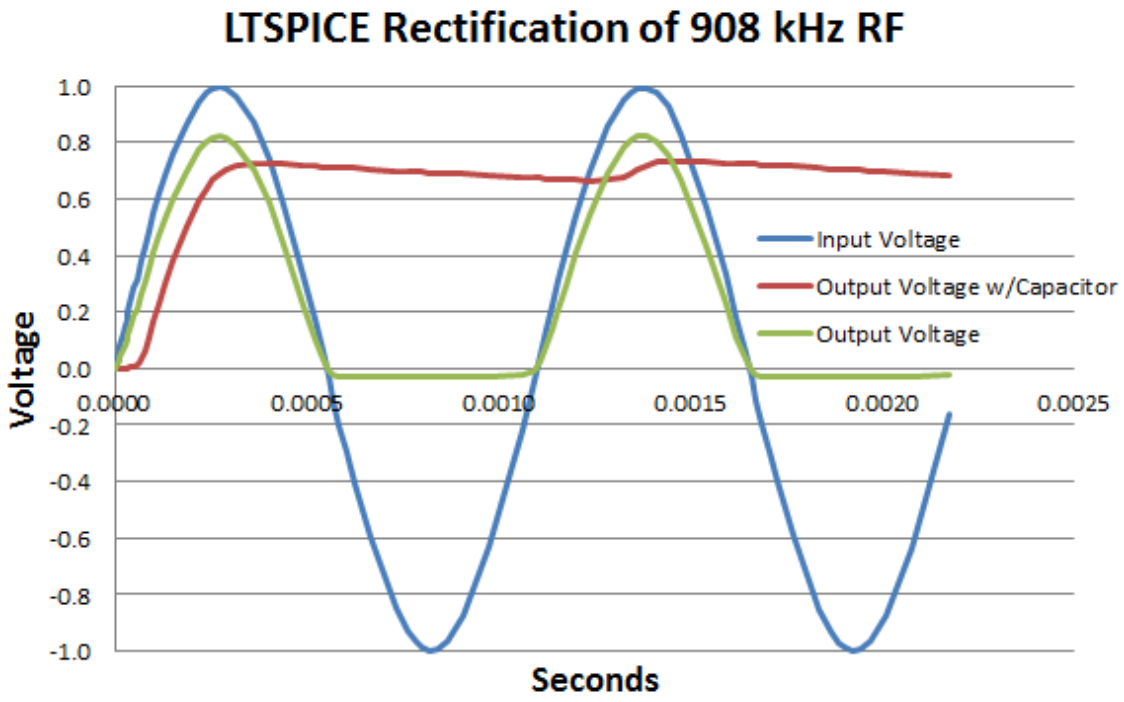

Figure 12. Results from the LTSPICE circuit in figure 4, the rectification of RF with a 1N5711 diode.

Figure 12 demonstrate the central need for the diode and the capacitor in combination for the rectification of RF to DC. The blue sinusoidal wave represents a 908 kHz carrier wave. The diode only allows for the positive voltage portion of the waveform to pass through it, and thus converts the alternating current to just positive current, i.e. direct current. Notice the loss of voltage in the green wave due to forward bias of the Schottky diode, another efficiency loss critical in converting weak RF to DC. Also this is a half wave rectifier, and thus another 50% is lost if only this circuit was used. The red line show the effect of a capacitor in line with the diode that store the voltage and thus converts the AC to almost pure DC.

The Villard rectifier is shown in the circuit diagram below, a slightly different configuration of diode and capacitor that allow the negative half wave to charge the capacitor and then the alternating forward voltage now being positive with respect to the diode is passed by the diode to form the red wave. In Figure 14, the output is sinusoidal but its voltage is above 0 V making it DC. While impractical because of it high ripple, it is the basis for the Villard voltage multiplier (VM) to come.

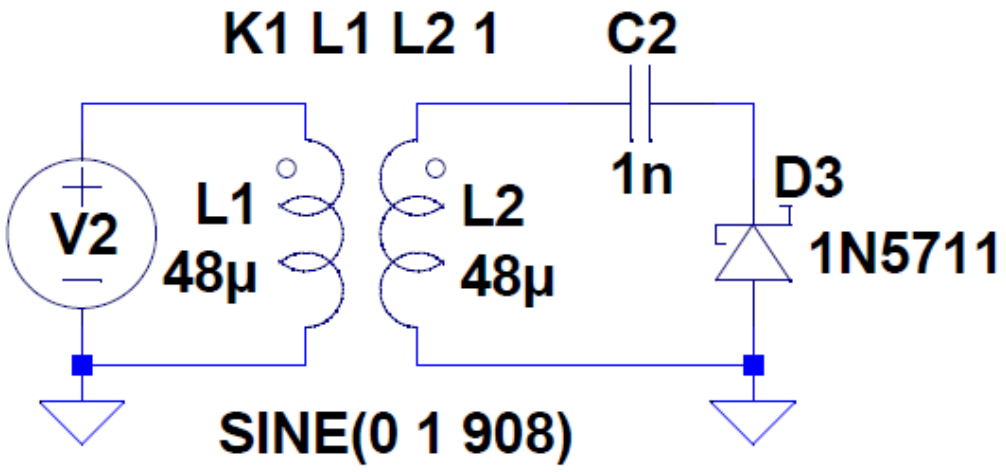

Figure 13. The Villard rectifier circuit has the capacitor before the diode and the diode positive is grounded.

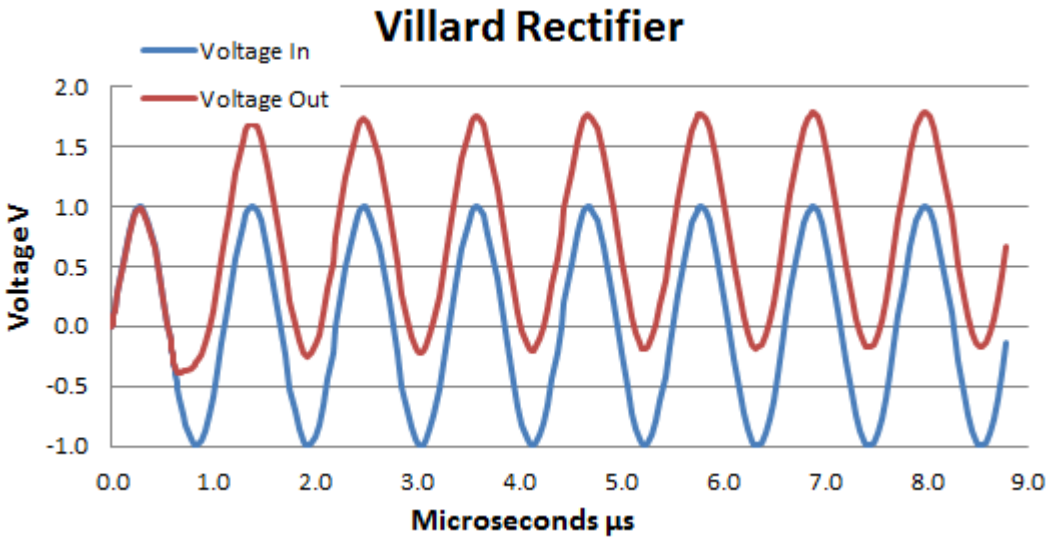

Figure 14. The output of the Villard rectifier is a sinusoidal waveform of positive voltage.

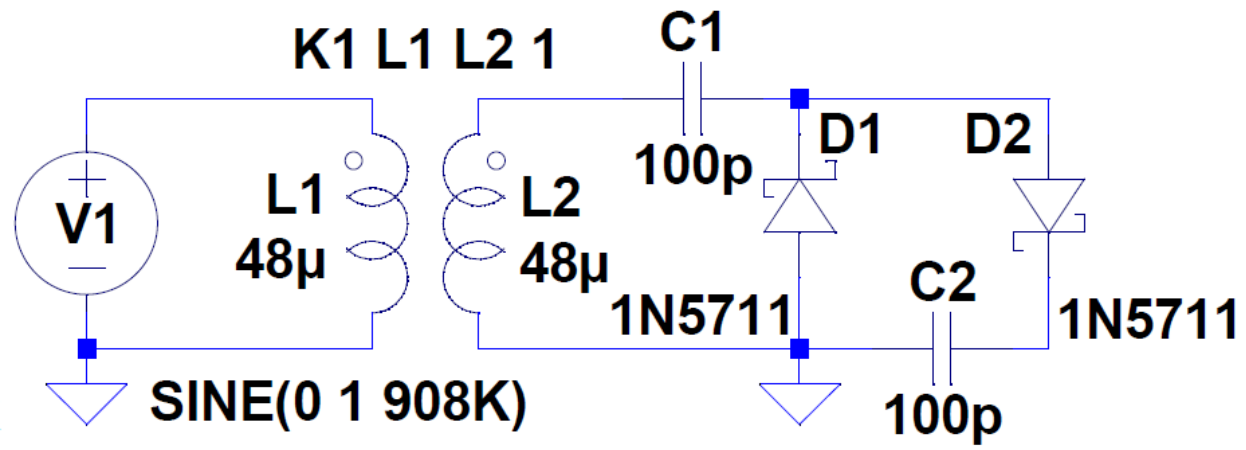

Figure 15. Villard Voltage Multiplier circuit with 1 stage.

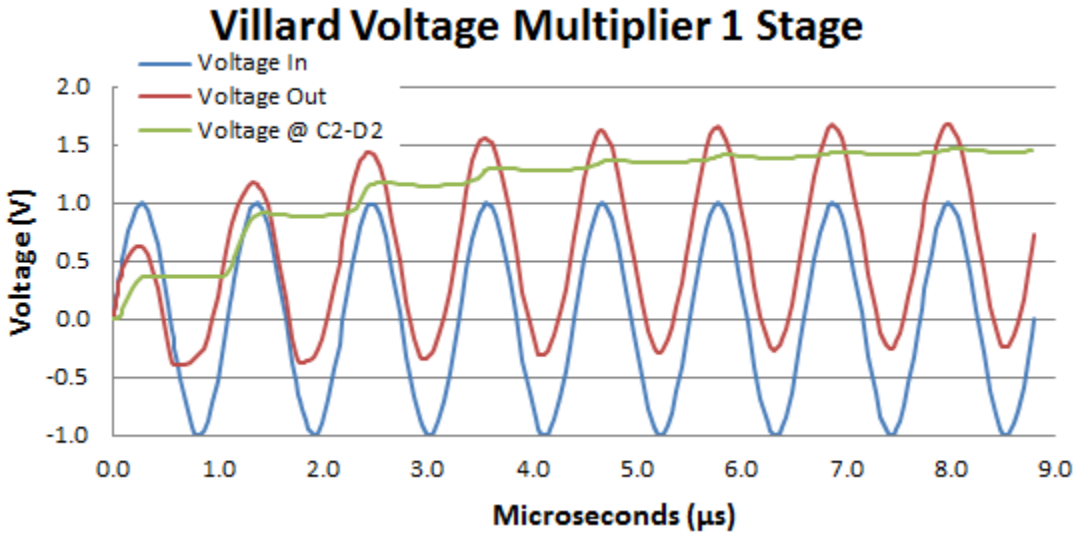

Figure 16. LTspice simulation of a one stage Villard voltage multiplier

The Villard voltage multiplier consists of a Villard rectifier with an adjacent capacitor and another parallel but reverse diode that effectively rectifies the positive sinusoidal wave and accumulates the charge on capacitor C2 smoothing out the ripple to a more practice DC current source, the green line in Figure 15. The Villard voltage multiplier became the basis for RF rectification for this project. VM voltage is equal to …

VM voltage output = $(V_p-V_{fd})*2N$

V_p is voltage peak for the input sine wave
V_{fd} is the forward voltage of the diode
N is the number of stages

For one stage the VM output should be (1-0.2)(2*1) = 1.6 V, and 10 stages =16V.

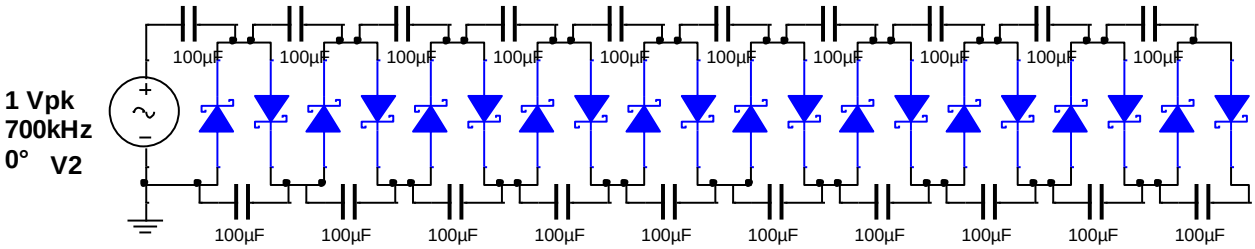

Figure 17. 10 Stage Villard voltage multiplier using 1N5819 diodes.

After quickly bread boarding a VM single and double stage, we developed a 10 stage VM using the Manhattan Technique for prototyping [11]. The Manhattan Technique was named after Manhattan Island, because the technique make heavy use of copper clad boards, cut into small pieces i.e. islands, that are glued onto a larger copper clad board that acts as a ground plane and the island as circuit nodes. The technique is a step up from solder-less wire plug-in-board, because the contacts are solidly soldered and the board contains a ground plane. The result is a prototype circuit board that can be mounted in an enclosure, and does not cost etching fees.

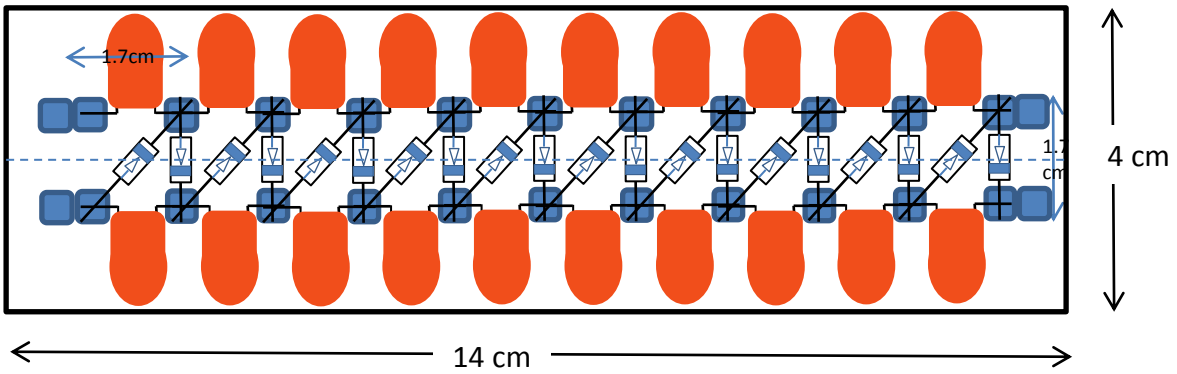

Figure 18. Manhattan technique board layout done using PowerPoint.

Figure 18 above shows the board design for the 10 stage Villard voltage multiplier. The blue squares are the copper clad board islands, the orange components are the Tantalum capacitors, and the diodes are shown between the lines of island nodes. The copper clad boards were purchased on eBay, and cut with a small metal shear to the size of the board and islands.

Figure 19. A 10 stage 1N5819 Villard voltage multiplier prototype made using the Manhattan technique.

In Figure 19, the islands were glued onto a copper board according to the layout plan. The islands being copper clad were easily soldered. The components were then soldered to these island nodes to produce circuit seen in the figure.

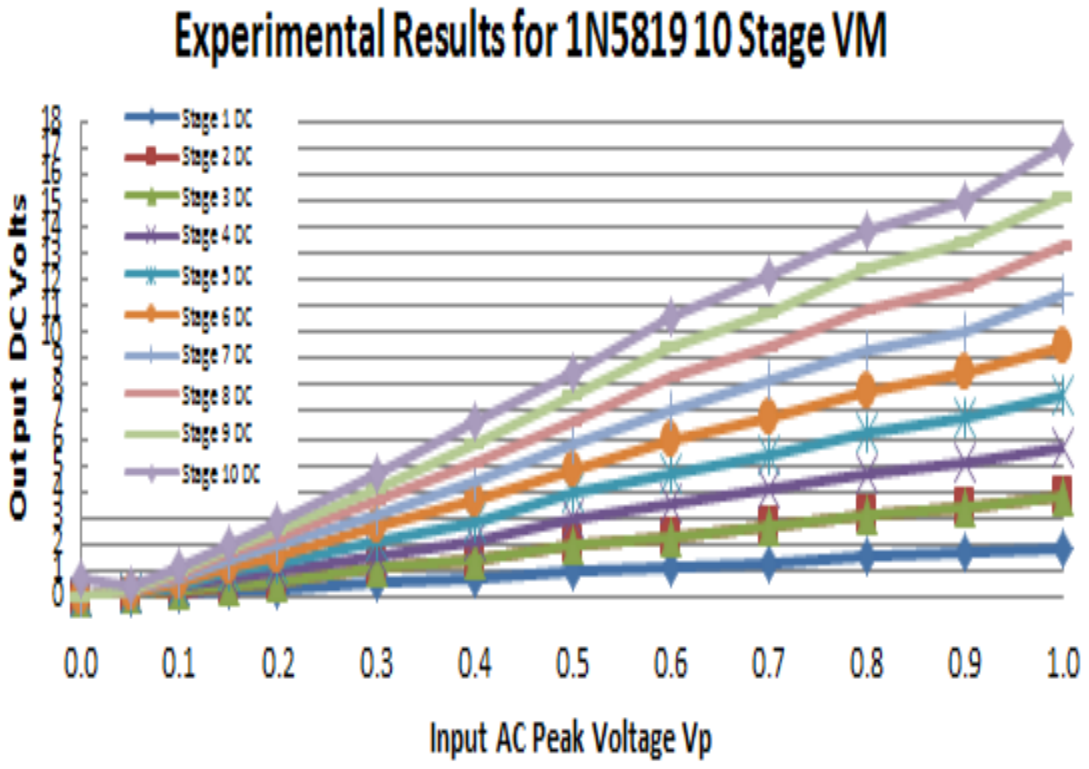

Figure 20. Experimental data plot of Vp input versus DC output using 1N5819.

Figure 20 data was obtained using a signal generator and monitoring the input with an oscilloscope to assure that the Vp input was accurate. While accurate, this does not account for Vp drop when using real RF source, a drop due to impedance mismatch or loading. Please note that stage 2 and stage 3 lines , green and maroon, overlap. Obtaining the same data from stage 2 and stage 3 was not expected, and must be due to bad components and/or connection. This was not realized until after we tried a new diode. In Figure 21, the 1N5819 voltage multiplier was simulated using LTSPICE software (SPICE electronic circuit simulation software provided by Linear Technologies) and the simulation results compared to experimental results to see if the same DC output should be theoretically expected or not. The plot indicates that the duplicate values were experimental error, and that in effect we really only had a 9 stage VM.

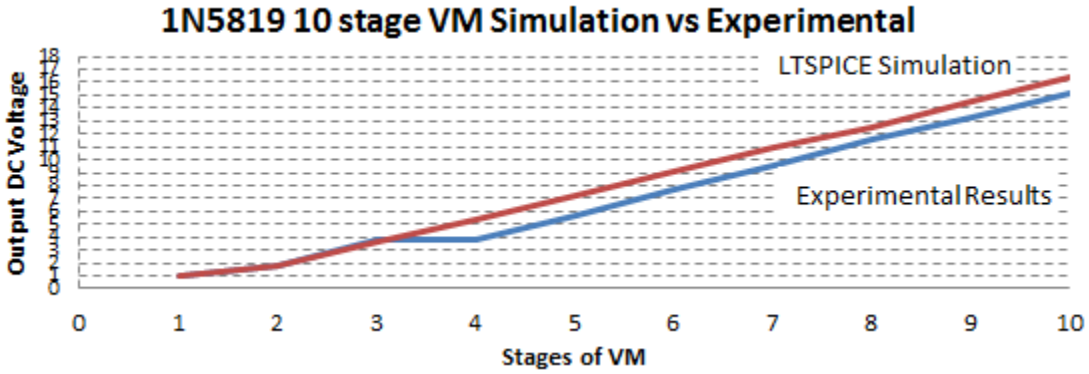

Figure 21. LTSPICE simulation results for 1N5819 VM versus the experimental results indicating a difference.

Some “DX” radio receivers that use diodes to rectify AM signals use parallel diodes to improve sensitivity. While these parallel diode designs exist on internet literature, professional literature could not be found to validate this concept. This project experimented with parallel diodes to lower its resistance, and thus provide better current. LTSPICE was used to simulate and compare the I-V characteristic of putting diodes in parallel. Figure 22 shows the LTSPICE simulation of the I-V characteristic of a 1N5711 diode put in multiple parallel combinations. The simulation show that greatest DC current jump per additional diode is from one to two diodes, so it may be cost effective. However, this does not analyze the effect on impedance at 908 KHz. This project compared a Villard VM made from single 1N5918 diodes with VM made from parallel 1N5711 diode to see if it would provide better rectification for weak signals.

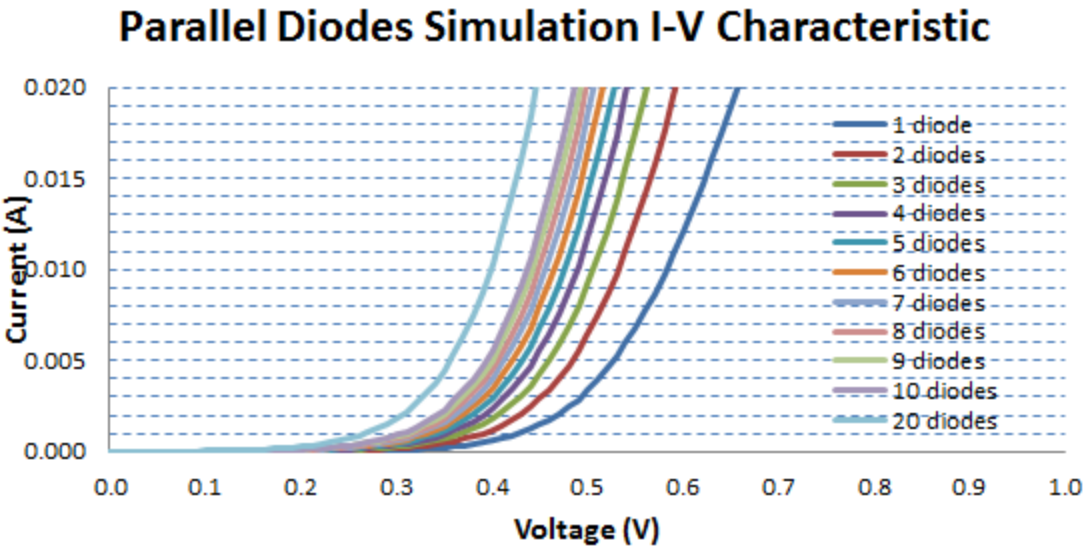

Figure 22. LT spice simulation of the effect of parallel diodes on their combined I-V characteristics.

10 STAGE VILLARD VOLTAGE MULTIPLIER

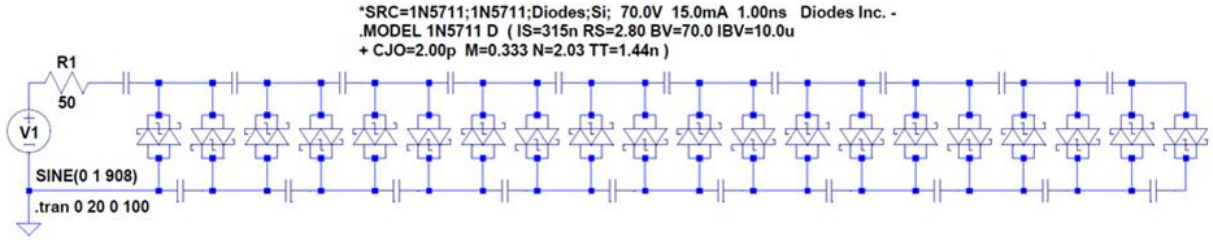

P PROTOTYPE BY MANHATTAN TECHNIQUE

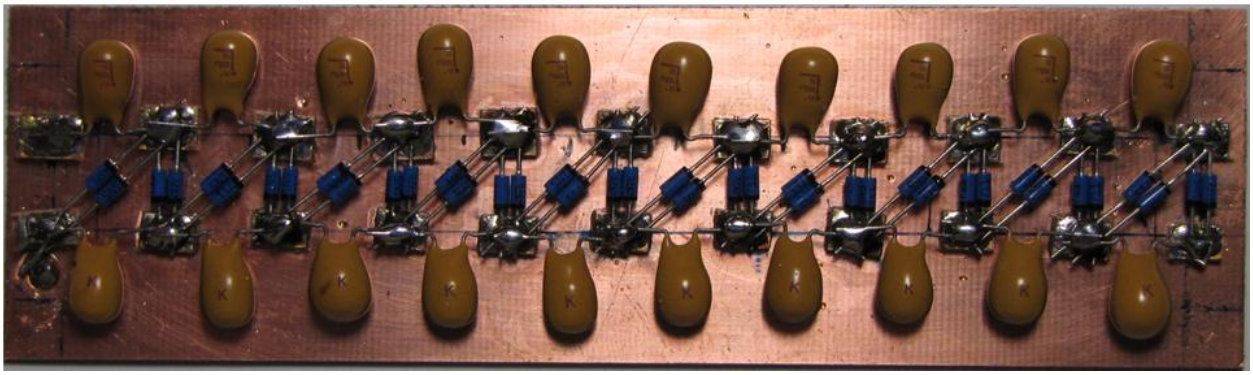

Figure 23. Circuit diagram of 1N5711 VM with parallel diodes and the circuit prototype made using the Manhattan technique.

Figure 23, the 10 stage VM was made using parallel 1N5711 diodes to see if parallel diodes would provide better current flow characteristics because the diode resistance would drop. The circuit was first simulated in LTSPICE. The impedance of the spiral loop antenna was measured using an Array Solutions AIM 4170 antenna analyzer at 724 ohms with 467 nH of inductance. That impedance was used in the simulations to predicted DC voltages at each stage. The 1N5711 parallel diode prototype board used Manhattan construction as shown in Figure 23. The

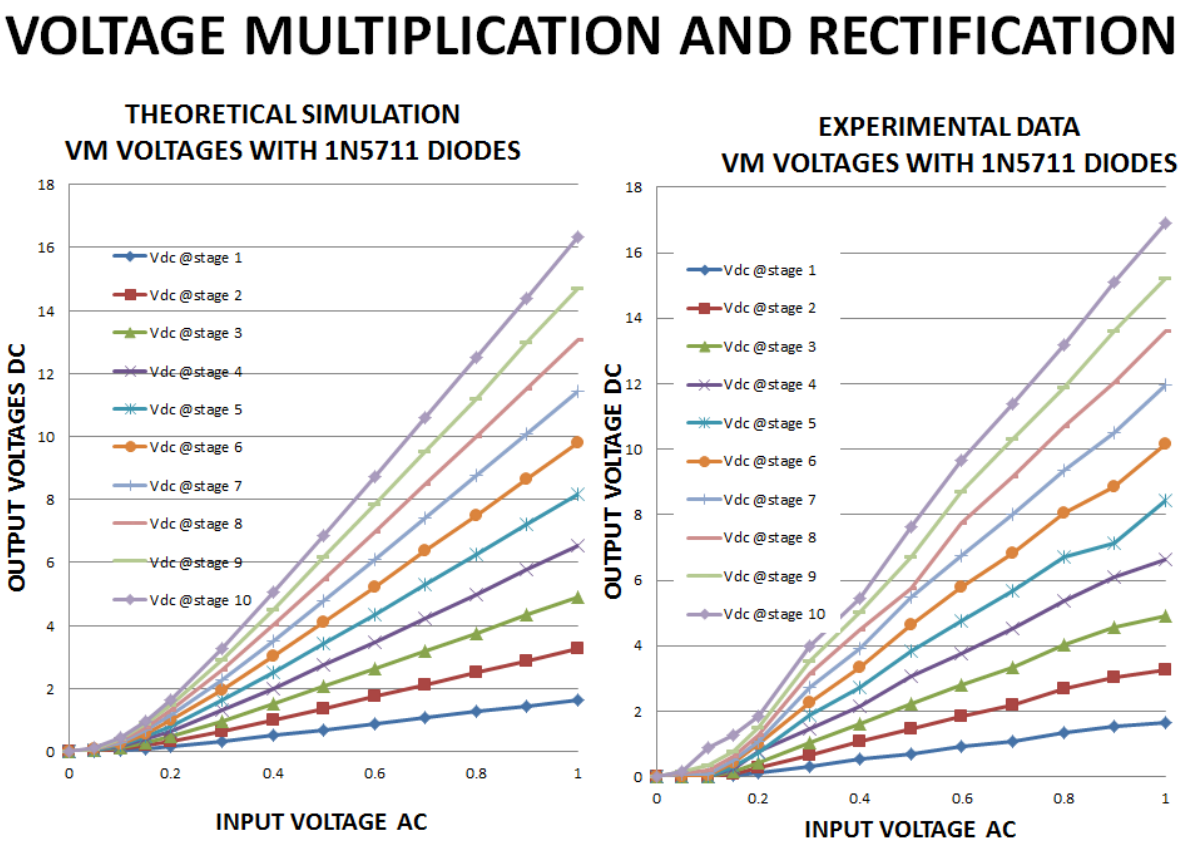

Figure 24. Comparison of 1N5711 VM simulation results versus experimental results.

In Figure 25, a signal generator was used to provide a 708 kHz signal into the 1N5711 VM prototype and the Vp was measured using an oscilloscope. DC measurements were taken at each stage of the VM. The experimental data was plotted on the right side of Figure 25 and the simulation data on the left. The simulation and experimental correlated closely. The experimental diodes seemed to give a slightly higher result than simulation diodes.

Figure 26 show the results from 10 VM simulations with the number of stages in the VM being the independent variable and charging current at 10 seconds being the dependent variable.

This was done because the question arose “if one only needs 4 stages to get the charging voltage needed for an application and the current is tapped at stage 4 off a 10 stage VM, do the unused stages lower the charging current.” In other words, what is better to use a fixed small number of stages or use 10 stages with the ability to tap off of various stages? The graph definitely shows that charging current drops of rapidly (exponentially) as the number of stages increase. Thus, once the voltage needed is obtained, there is no advantage in increasing the stages. Simulations were also run using a 10 stage VM tapped at 3, 4, and 5, and the theoretical charging currents measured. The red squares in the graph are currents associated with a tapped 10 stage VM scenario. Looking at this graph in figure 18, one can see that following unused stages do lower the charging current, slightly 15% to 9%, in the simulations. So yes, extraneous stages do have a negative effect, but I decided to use a 10 stage tapped circuit at the cost of a slight charging current loss in order to have the advantage of tuning the stages to obtain the voltage needed for the application. Other researcher have used a DC to DC conversion chip to obtain this same tuneability, but that too will have an insertion loss.

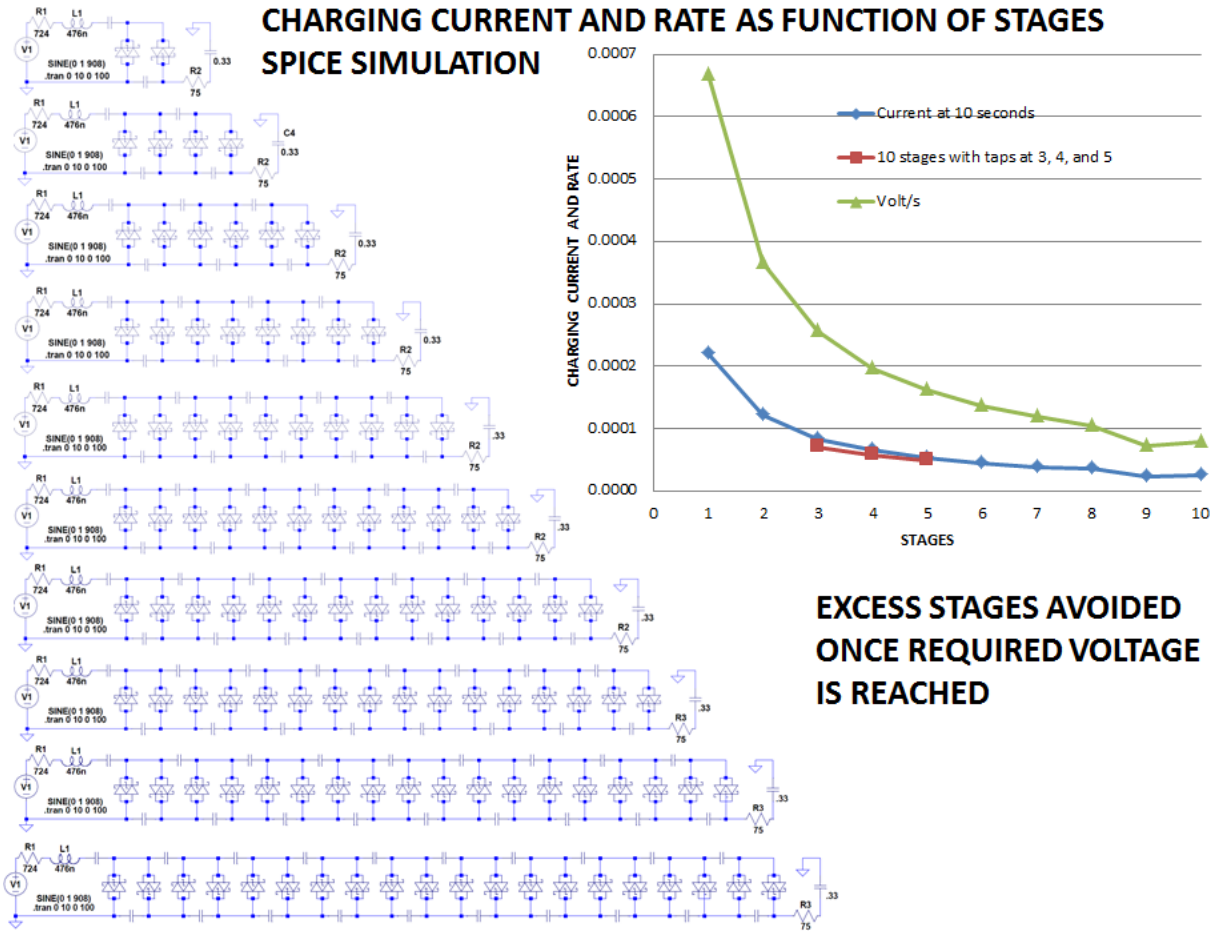

Figure 25. Individual simulations of VMs from 1 stage to 10 stages measuring charging current to super capacitor.

Figure 27 shows the circuit diagram and enclosure used to test this harvester. A 10 point rotary switch was used to tap current and voltage off of selected stages. The 100 uF Tantalum capacitors were rated at 16V so a 15.1 V Zener diode was placed between the last stage and ground to clamp voltage below the point of damaging capacitors. Another Zener diode at 5.5 V was place between the super capacitor and ground to clamp the charging voltage at a safe level. A 50 µA meter was installed and used with 1 stage to measure the current coming from the antenna to aid in tuning the antenna to the strongest radio signal. A 0.33 µF super capacitor was placed in the holder to the left on the picture. The enclosure has 3 pair of banana jacks on the side (not shown in the picture) that allows for the monitoring of VM and super capacitor voltage and the monitoring of super capacitor current. This system was tested using a laboratory source of RF signal from a Ramsey transmitter couple to the loop antenna through a coupling loop. The capacitor readily charged and could be used for the application described in the next section.

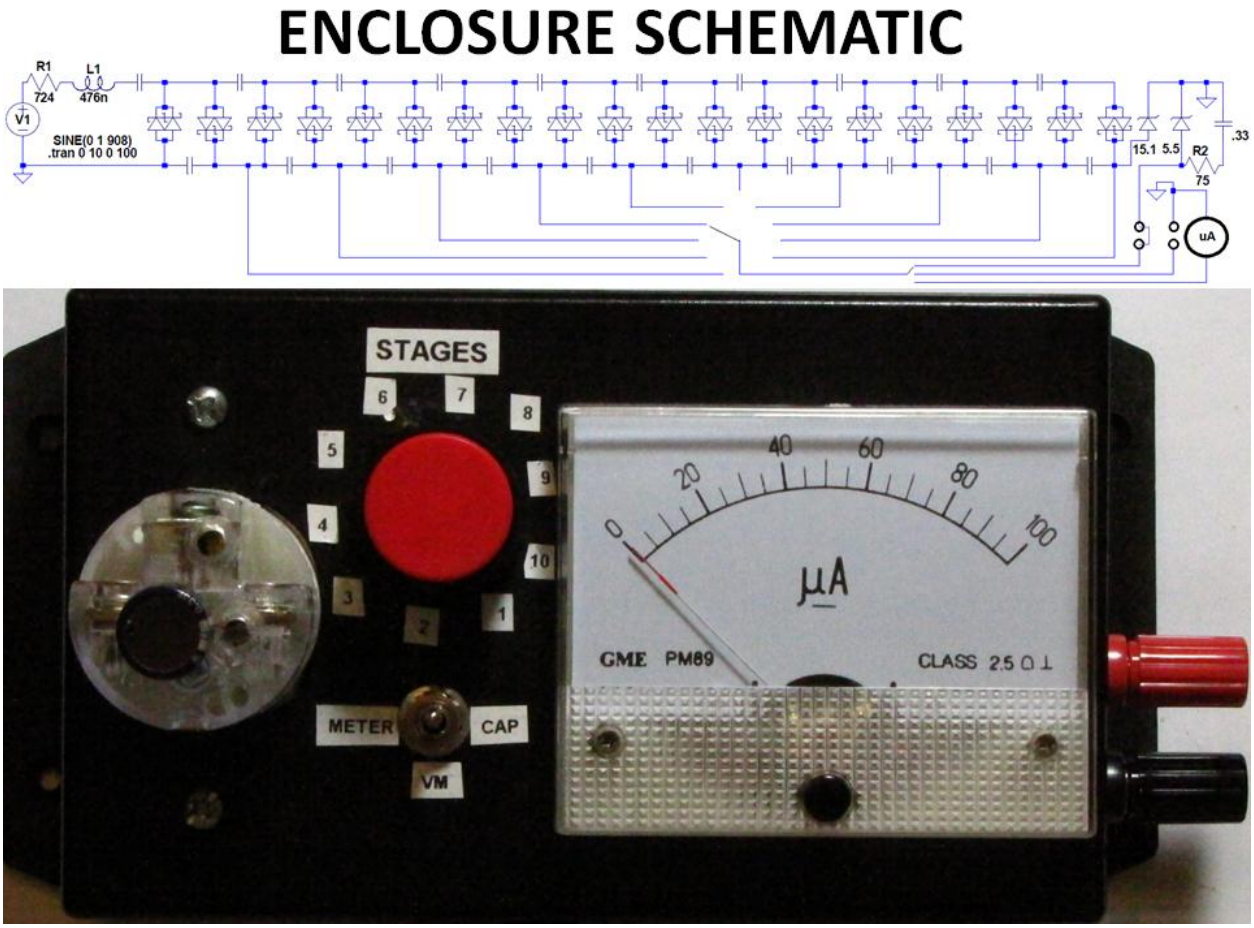

Figure 26. Figure 27. RF energy harvester circuit and enclosure picture.

3.1. VM conclusions

The 1N5818 made a better VM than the 1N5711, because it had a lower forward voltage that provided more sensitivity than the 1N5711 with parallel diode. The forward voltage characteristics of the diode are more important that it's internal resistance. It was best to choose the minimum number of staged necessary to obtain final charging voltage, because the charging current diminishes exponentially with the increase of stages. LTSPICE software provided accurate predictions for a 908 KHz signal in the VM development.

The project has a lot more experiments before it is ready to be put into a printed circuit; however the Manhattan technique has proven to be an effective way of prototype to get to that point.

3.2. VM discussion

While enough data was collected in the laboratory from near field laboratory generated RF to make conclusions on the VM, we never collected enough RF data from nearby radio stations to characterize the harvester with statistical significance for weak signals. We ran out of time. Future experiments would be to harvest local weak signals. Several experiments that could be done would be t 1) see if parallel diodes using the 1N5819 would be more sensitive than the 1N5819 was 2) try larger antennas, albeit loop or long-wire, and 3) use a full wave voltage multiplier. A 5 stage full-wave VM may have been better than a 10 stage half-wave VM for the requirements of this weak RF signal project, because while using the same number of components it would deliver the voltage multiplication of a 10 stage VM in 5 stages. But, we have no data to support that hypothesis. However, weak signal sensitivity was a paramount issue with the goal of this project.

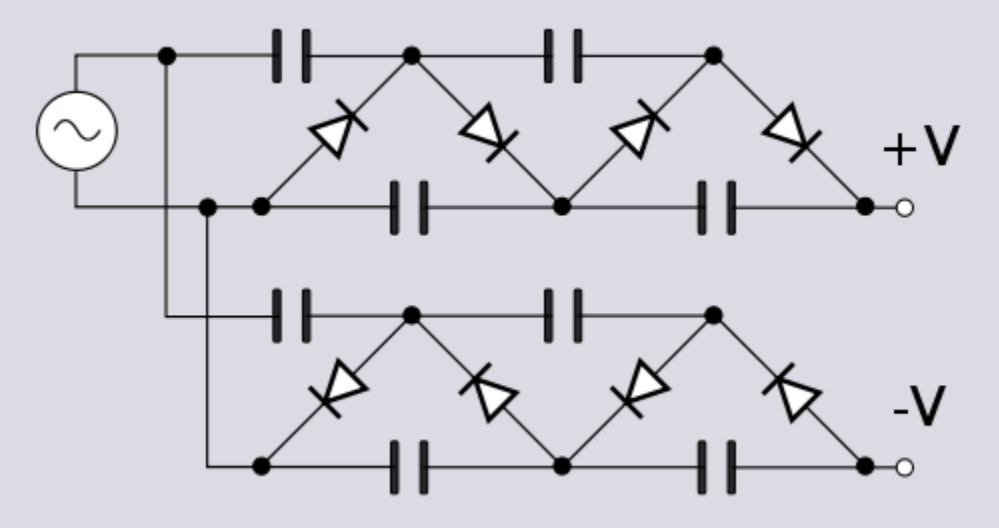

Figure 27. Full wave Villard voltage multiplier found in Wikipedia.

The 10 stage VM with taps at each stage was preferred over lower fixed stage VM, even though tapping is less efficient than using a fixed number of stages, because the tapped system seems to be tunable to signal input amplitude. Three or four stages may not provide enough voltage

from a weak radio station, whereas a tunable 10 may be tuned up to give more voltage. More data needs to be collect to test this hypothesis

While the goal was to develop a completely passive RF energy collector, one experiment would be to use a microprocessor to control the system after an initial boot up charge was collector. The microcontroller could eventually monitor voltage and even switch between capacitors after one had been charged. It would be interesting to see if forward biasing, adding a DC voltage across the diode to compensate for the forward voltage barrier, would provide better sensitivity for weak stations or just increase the charging rate. With microcontroller control, it may be possible to alternate charging of several super capacitors and switch them to series connections to increase output voltage (most super capacitors are limited to 5.5 volts).

4. Energy Storage Using Super Capacitor

Energy is a very precious resource. Quoting a TI engineer: "Every joule wasted from the battery is a joule you will never get back" [12]. Finding a way to store energy has been a problem for years due to the cost and size of batteries. New technology such as super capacitor has been out recently and hoping to replace or being another energy storage alternative. While the technology is still fairly new, we attempted to use this new technology in this project to benefit our needs.

Energy storage is a critical part of the project as the harvester can only harvest a very small amount of energy. Storing the energy and accumulating it to a usable energy level had become a problem that we needed to solve.

A way we came up with storing the energy was to use a super capacitor as our storage device. Super capacitor offers a few advantages that favor our conditions versus a lithium-ion battery or regular capacitor.

4.1. Background

Capacitor, previously known as condenser, was invented by a German scientist named Ewald Georg von Kleist in 1745 [12]. The use of capacitor was not common till the invention of radio in the 20th centuries. Radio created the demand for capacitor, which it was used to tune the radio to achieve higher frequencies with higher capacitance and lower inductance. Other uses of capacitor include power conditioning, power factor correction, noise filter, smoothing the output of power supplies, and power storage.

Super capacitor, or electric double-layer capacitor, is an electrochemical capacitor with relatively high energy density, usually hundreds of times greater than regular capacitor. Super capacitor was invited in 1957 by General Electric. The uses of super capacitor are widely seen on automotives; where it is used to jump start an electric car.

Lithium-ion battery is a type of rechargeable battery where the ion moves from the negative electrode to the positive electrode during a discharge and the opposite during a recharge [14]. It is commonly used in consumer electronics such as laptop, cell phone, digital cameras etc.

4.2. Storage device

The requirement for this project was that the energy storage device needs to be able to accept a wide range of voltages instead of requiring a fixed voltage. A few energy storage candidates have been considered to examine their advantages and disadvantages to select the best one for this project. The candidates are: lithium-ion battery, regular capacitor, and super capacitor. Below is a brief list of their advantages and disadvantages for the purpose of this project [15].

Table 3. Advantages and disadvantages of storage devices.

Type	Advantages	Disadvantages
Lithium-Ion	High specific energy density Relatively low self-discharge No memory Wide variety of sizes and shapes	Require protection circuit for charging Life degrade over time High internal resistance
Regular Capacitor	Cheap Many different types and materials High maximum voltage Variety ESR selection	Low specific energy/power density High self-discharge rate
Super Capacitor	High specific power density High capacitance Short charge time Long life cycle Low ESR Low leakage	Low overall specific energy density, relatively high versus regular capacitor Low maximum voltage Higher cost

Selecting the best energy storage device is critical to this project; it determines the possibility and expandability of our application. Knowing how much energy being able to harvest and accumulate would help us scale our application. From the comparison chart, lithium-ion have the most specific energy density, which allowing us to power an application for a long time. However, lithium-ion can only accept a fixed voltage and current source for charging, and while the RF strength in the air can varies, it would be very difficult to ensure a reliable charging source. Thus we have ruled out to not use lithium-ion.

Figure 28. Lithium Ion Battery

Figure 29. Electrolytic Capacitor

Regular capacitor was another option we have considered. It is cheap and comes in varieties of sizes and materials. An advantage of regular capacitor is it accepts a wild range of voltages, as high as kilo-volts. It eliminates the need of protecting and charging circuits. However, regular capacitors have a relatively high leakage rate, where in

some cases it would leak out as much as it was charging. A special type of capacitor called the tantalum electrolytic can reduce the leakage dramatically, but the capacitance of a tantalum electrolytic is too small in comparison with other capacitors. A big capacitance size tantalum electrolytic capacitor was out of the equation due to the cost was more than our budget allowed. Another problem is they do not provide good specific energy for application uses.

On the other hand, super capacitor was chosen to be our storage device due to its advantages matches our project's need. Super capacitor has a higher specific power density and higher capacitance than regular capacitor, allowing a greater storage space with a minimum of 0.33 farad. Super capacitor also has an extreme low ESR (Equivalent Series Resistance) for faster charging. The electrical principle is voltage equals to current times resistance; with a high voltage and small resistance, it results a higher current, thus fasting the charging on the super capacitor. Another advantage of super capacitor is the low leakage rate. It can retain the charge for days without losing much of its charge, but the super capacitor must go through "memory" training. This memory is called the dielectric absorption or soakage [13]. This occurs when fully discharged a capacitor and left without applying voltage or shorting the thermals, the capacitor will gradually establish a charge in itself to a fraction of its original charge. The memory training is a series of charging and discharging performed on the super capacitor. Charging the super capacitor to 90% of its rated voltage and then discharge, then repeat the process 3 times. The memory training will help reduce leakage loss and getting "free" charges back in some way. Although super capacitor has a lower specific energy density versus a lithium-ion battery, the application we are using should still be able to run without discharging too much from the super capacitor.

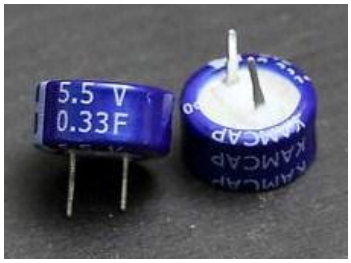

Figure 30. Super Capacitors

A super capacitor charger IC (Integrated Circuit) was examined to further the charging efficiency and overall reliability. The IC was Linear Technology's LTC4425, a programmable current limited charger IC [16]. It is designed to have a consistence charge to the super capacitor from a lithium battery, USB, or a 2.7V to 5.5V current limited power supply. We ruled out this IC in our design. The IC itself requires some power to activate, which it will draw power from the harvester.

A simple way to regulate the charging on the super capacitor can be done by using a zener diode rated at 4.8V. As soon as the voltage gets above the breakdown voltage, it will become reverse biased and it will short to the ground to stop charging the super capacitor [17]. Using a zener diode as a voltage regulation device may seem to be lousy and unreliable when compared to a voltage regulator. However, since the super capacitor can accepts any voltages below its rated voltage, we would only need to worry about it being overvoltage and not under-voltage. A zener diode will regulate the upper voltage limit on our super capacitor while it allows any voltages below the limit to pass to charge the super capacitor. A voltage regulator can be used to give a constant voltage output source if the input voltage is above the dropout voltage. A dropout voltage is the minimum voltage differences between the input and the output of the voltage regulator, and in order for the voltage regulator to work, the input voltage must be above the dropout voltage. Also, if the input voltage is higher than the regulator can handle, it will damage the voltage regulator. Since the RF signal can varies from

time and location factors, there is no guarantee to have a stable input signal. Thus simply limiting the upper limit voltage using a zener diode was the best approach for our design. One drawback with the zener is that it couldn't limit the excesses current, but RF signal received from our antenna is going to be very small unless we are right next to a powerful transmitter to induce the power density loss, otherwise current should not be a problem. A robust design should and will be considered to optimize the charging technique.

Here we take a look at the charging curve of the super capacitor using a 3-stages voltage multiplier [18].

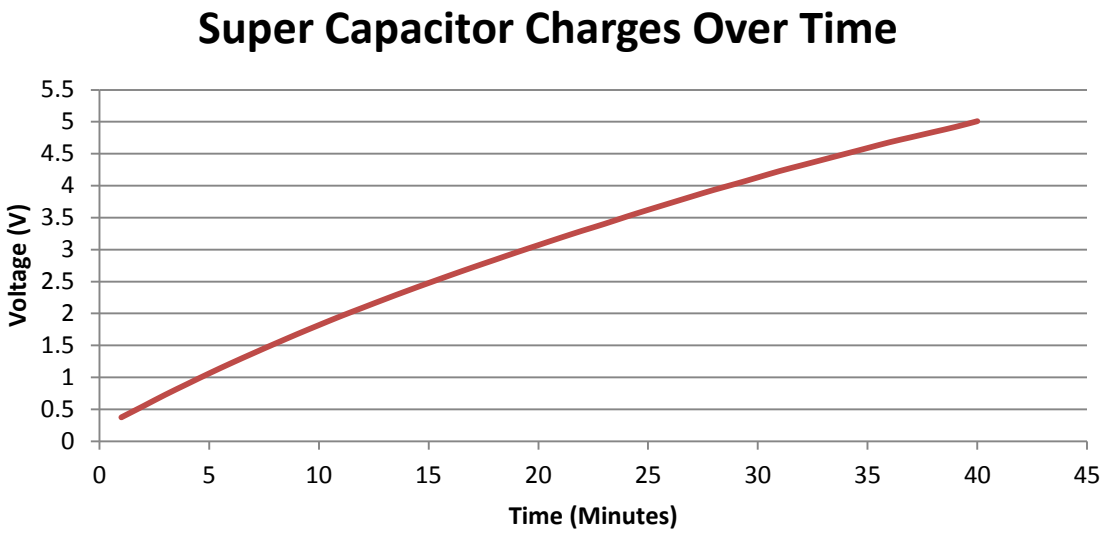

Figure 31. Super capacitor charging curve using 3-stages voltage multiplier

The charging curve seems to be rather linear instead of a progression of a 5RC time constant.

The calculated RC time constant is 16.5 seconds using the equation t = R * C, where R is the resistance in ohms and C is capacitance in farad. The resistance used in this calculation was the 50 ohms ESR, and the capacitance was 0.33F. As we can see the charging curve above and compared with the calculation, the numbers doesn't quite seem to match with the curve. The RC time constant would be an ideal charge time for the super capacitor, however, the actual charge time was much longer. Due to time constraint, we do not have additional researches to figure out why wasn't the charge on the super capacitor follows the RC time constant. A simple yet to verify guess was that the voltage multiplier was not optimized for the super capacitor. As shown previously on the antenna output with and without the voltage multiplier, the voltage multiplier shifted the antenna output and even lowered the Q factor of the antenna. The basic principle of a voltage multiplier is the trade-off between voltage and current. The higher the voltage means the lower the current, and vice versa. In this case, the voltage multiplier might have had a hard time providing the current the super capacitor wants. Study shown that super capacitor is capable of drawing as much current as it can get in a short time. The voltage multiplier was probably bottlenecking the super capacitor's charge, thus we see a linear charge

curve instead of an exponential curve. Once again, this explanation was based on our knowledge on the concept, a scientific method and measurement should be experimented when time is permitted.

4.3. Improvement

There was one improvement can be done for this part of the design. The improvement was having a robust charging circuit that could protect the super capacitor from being overcharged while it does not take away much of the harvested energy. A low dropout voltage regulator from TI could be an alternative to make this improvement.

We were able to charge the super capacitor using RF generated energy up to 5V in a reasonable time using a lab generated RF signal. The super capacitor then switched to our application and was able to power the application for a short period of time.

5. Low Power Application

Low power devices and ICs have always been a hot topic and where the technology trend is moving forward to. Moore's law predicts that the number of transistors that can be placed on an IC doubles approximately every two years. This prediction has been true for years, and the transistors inside an IC are getting smaller and smaller. At the same time, voltage required to run the IC are also getting smaller. Cell phones that run on 3.7V battery, processors that can run under a voltage are examples of low power applications. In this project, we attempted to run a lower power application off RF harvested energy.

Low power application utilizing RF harvested power to demonstrate self substantially. Power harvested from the RF harvester is very minimal. The amount of energy can be harvested and stored is critical to the application. Without much energy to deal with, our application must consume as low power as possible. Most modem applications required a decent amount of energy to run. A standard 5V is required on most applications or even 12V in some cases where the microcontroller is supplying the 5V rail to the components. With the voltage multiplier we have, voltage isn't our biggest concern; we can easily step up the voltage to the required voltage for the application. However, the amount of current it consumes is our biggest problem.

Based on the power consumption requirement, we had chosen TI's (Texas's Instruments) eZ430-RF2500 development kit. The kit includes two dongles; each dongle has a low power microcontroller MSP430 and a CC2500 transceiver [19]. One dongle has an extra component for the USB interface to the computer. It acts as a software emulator to allow programs to load into the MSP430. It also acts as a data bus for the computer to receive data from the MSP430.

5.1. The MSP430

MSP430 is TI's ultra low power value line product. It is a 16-bit microcontroller featured with 10-bit ADC resolutions and two 16-bit timers [20]. The selling features of this microcontroller are the power consumption modes. According to the specification, the MSP430 can operate at 2.2 volts with a minimum of 120uA. The lowest power mode or the LPM3 consume about 0.7uA at 2.2V.

5.2. The CC2500

CC2500 is TI's low-cost 2.4GHz transceiver. It features with OOK, 2-FSK, GFSK, and MSK modulations operating between 2400 to 2483.5MHz [19]. The CC2500 has a programmable output power up to 1 dBm and programmable data rate from 1.2 to 500 kBuad. The operating voltage is between 1.8V to 3.6V and the current consumption during sleep mode is about 400nA.

5.3. The application

The idea of our application was to use RF harvested energy to power a low power device(s) and sends data wirelessly. Imagine an environmental sensor out in the desert or the wilderness that is constantly sampling data and sends the data back to the receiver. This sensor would need a reliable power source and with minimum care as possible. Using a standard battery, it would require a replacement whenever the battery runs out of power. However, if using RF harvested energy, the sensor would never run out of power as long as the RF is broadcasting, and it would not require a user or technician out to the field to replace the power source.

The purpose of our application was to sense the ambient temperature around the device and measure the supply voltage and then sends the data back to the computer via Wi-Fi transmission. It is done by using MSP430's internal analog-to-digital converter to sample the ambient temperature and as well as sample the supply voltage. The data then patch into transmission packages to the CC2500 to transmit and receive.

5.4. Hardware

A simple hardware overview is shown below.

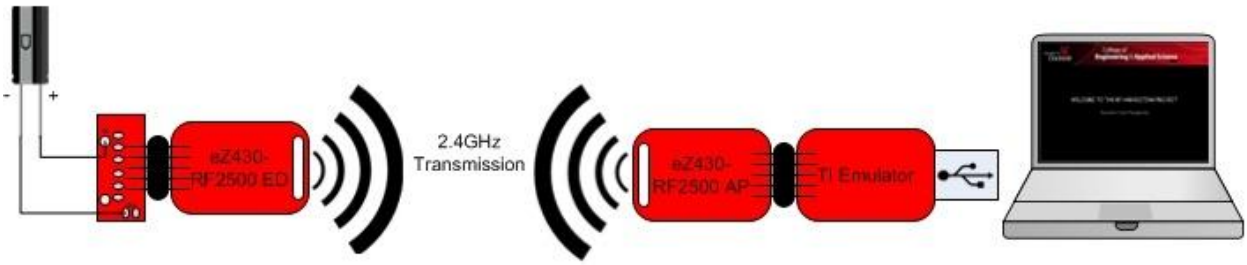

Figure 32. Application Overview

The left side of the diagram is the End Point (EP) dongle, attached and supplied by the super capacitor. The right side is the Access Point (AP) dongle, attached to the USB emulator and interface to the computer. The charge on the super capacitor was between 2.2V to 3.6V, any voltages below or above that range would not work, especially above the 3.8V threshold; it would damage the MSP430 permanently. If the voltage is below the operating voltage of 1.8V, the MSP430 simply won't run without any permanent damage. However, to truly being able to run this application, a minimum of 2.2V was required due to the internal 16-bit timer required 2.2V and as well as the CC2500 required a bit more voltage than the 1.8V MSP430.

According to the specification of the kit, the wireless communication range is roughly 50 feet on line-of-sight. Though 50 feet might not be as useful when it comes to wilderness, but the AP can serve as a data hub to receive and transmit to another data hub and so on, thus making long distance communication a possibility. However, this experiment has not yet been done, but theoretically do-able.

5.5. Software

The operation of the application is shown below in a flow chart diagram.

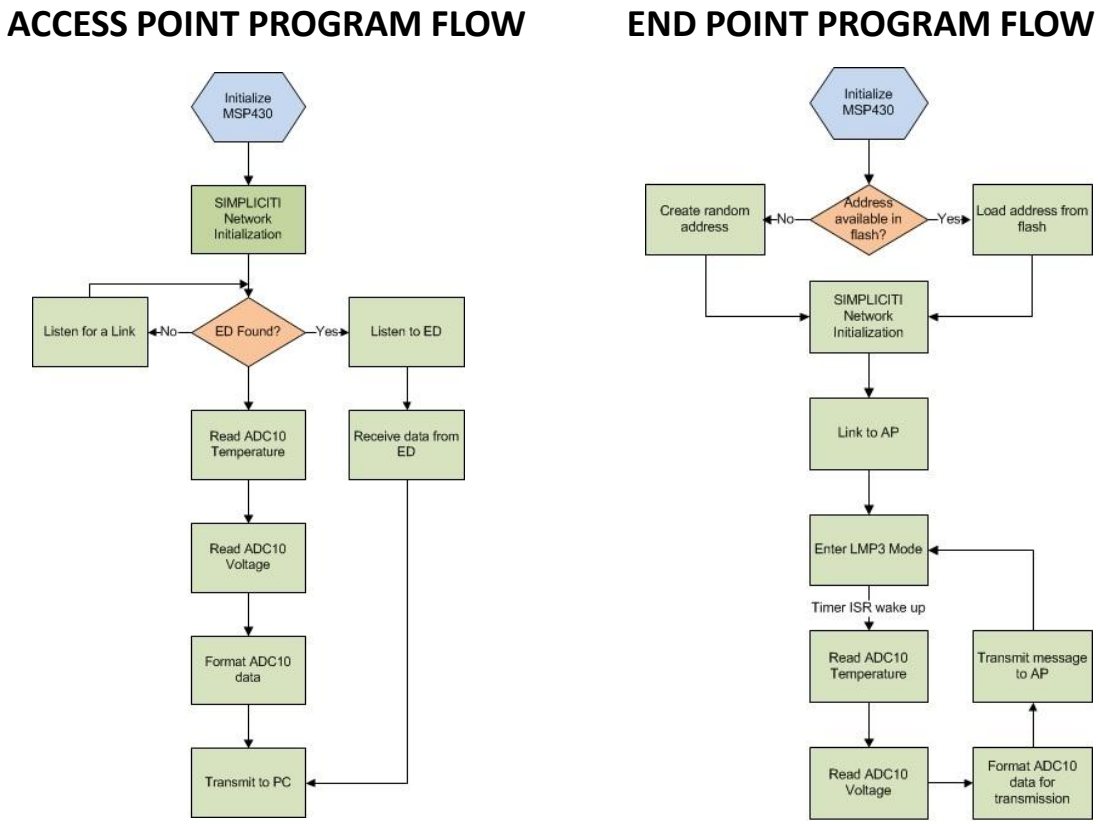

Figure 33. Program Flow Chart for AP and EP.

The above flow chart shows the program flow for both dongles. The dongle that was connected to the computer is called the Access Point and the dongle that was out in the field is called the End Point. The Access Point (AP) act as a data hub, it can support multiple End Point (EP) devices and receive data to the computer via the USB interface. The EP act as the sensor that will read the temperature and voltage in our application.

The operation of the AP is shown on the left side of the flow chart. When powered on, the MSP430 does self-initialization to get it ready for the network initialization. The network

protocol used in this kit is called simpliciTI, a proprietary protocol made by TI for their wireless IC. After network initialization, the AP began to search for EP(s) for link-up. If no EP found, the AP then proceed to initializing the internal analog-to-digital converter for temperature and voltage measurement. If EP was found, AP would listen for packages from EP and sends acknowledgment back to EP. If no package received, AP continues to take measurements. With the measurements made, the AP formats the data and sends it out to the computer via the USB interface at a fixed baud rate of 9600 bps.

The operation of the EP is shown on the right side of the flow chart. Again, when powered on, MSP430 does a self-initialization. It then looks up its flash memory for wireless address. If no address found, it then creates a random address for communication. If address found, proceed to use the presenting address for communication. With the wireless address, EP initializes simpliciTI for networking with the AP. As soon as linkage between the AP and the EP is established, EP then initializes the internal analog-to-digital convert and takes sample of the temperature and voltage. EP reformats the data and sends the data to AP for display. It then goes into low power mode 3 (LPM3) for about 5 seconds and wakes up to take measurement again, and so on. Low power mode 3 is MSP430's second lowest power mode, it consumes about 0.7uA at 2.2V.

5.6. User interface and display

A user interface and display was developed for this application. A data displaying view of the interface and display is shown below.

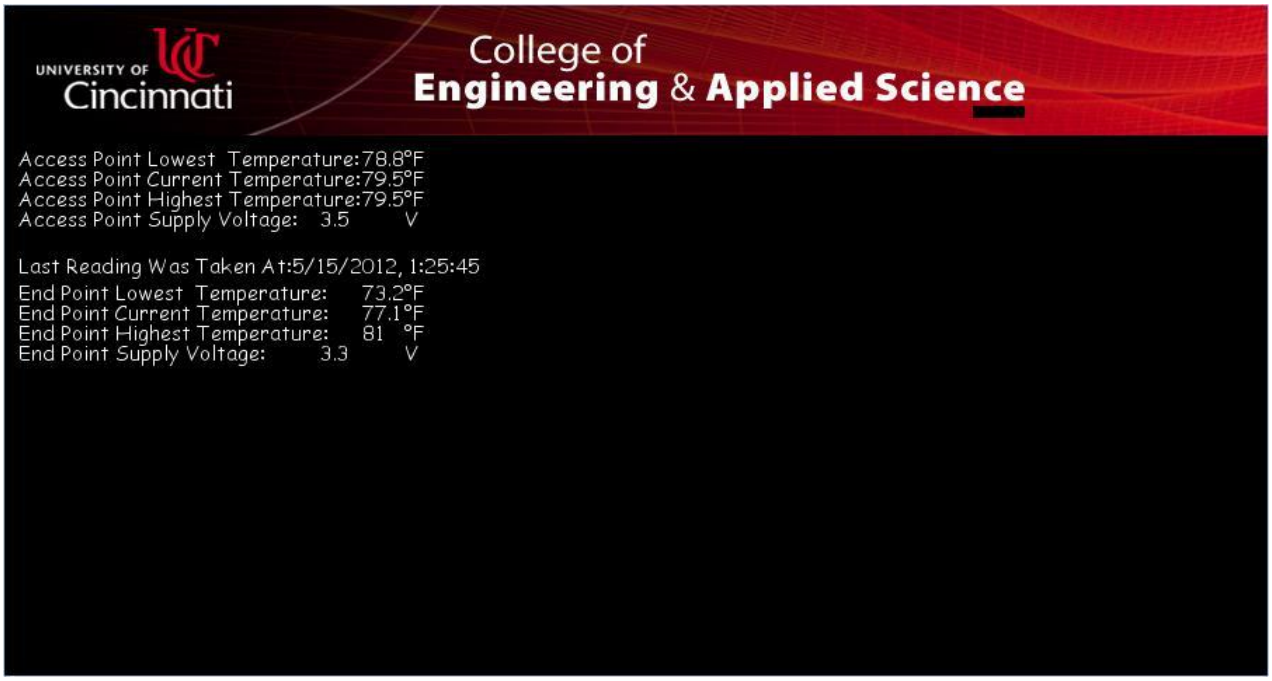

Figure 34. Application GUI

This user interface and display was developed using a programming language called Processing [21]. It is much similar to C/C++, except with its own libraries, syntaxes, and program flow.

The display shows the access point and end point temperature and voltage readings. It calculates the lowest, current, and highest temperatures throughout all the measurements made. A time stamp will be created whenever the program received data from EP. This was because the EP goes into sleep mode for 5 seconds every time after measurements. It is also because the EP will be supplied by the super capacitor, if for some reasons that the super capacitor is drained or the power to the End Point has been lost, we would still get the last known temperature and voltages, and know the time when the EP stopped working.

A simple program flow for the interface and display is shown below.

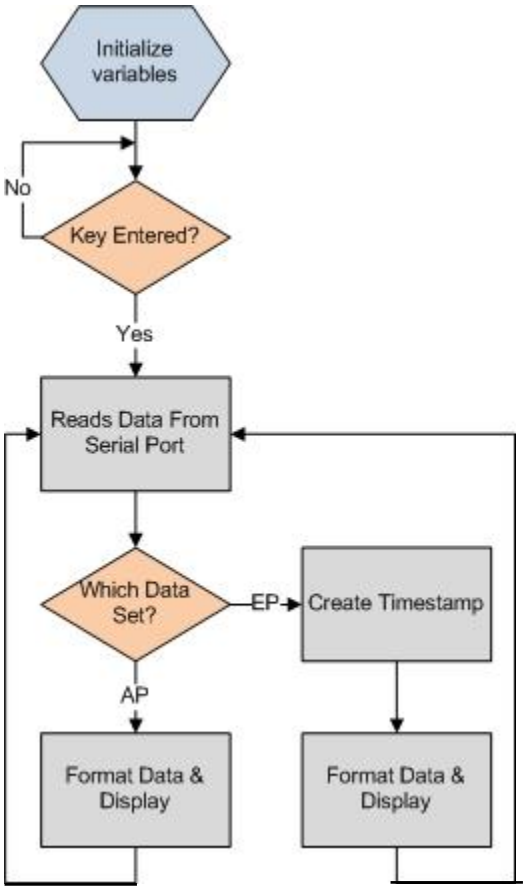

Figure 35. Interface & Display Program Flow

The interface and display program first initialize key variables that were used throughout the program. Then it prompts the user to enter a key to begin the data processing stage. When the program reads data from the serial port, it decodes the data string and determines whether it was AP or EP data. If data are from AP, the program formats the string and displays them on the screen. If data are from EP, a timestamp will be created at the time of data reception. The

program then follows a similar data format and displays the temperature and voltage on the screen.

5.7. Improvements

There are improvements needed to be done to make this application more robust. Some of the improvements were considered during the design of this project, but due to time constraint, they were not implemented in the project and they are the top priorities on the agenda when permitted by time.

The first improvement we had looked at was on the hardware side. As it was mentioned above, the safe operating voltage for the dongle was from 2.2V to 3.8V. The dongle itself does not have a voltage regulator or any protection circuit. If the super capacitor's charge voltage ever got above 3.8V, then the dongle is in risk of being damaged. A simple solution we had looked at was using a zener diode to clamp the voltage below 3.5V. However, a zener diode is not a safe and good way to regulate voltages, as it has noise and it is current depended as well. Another option we had looked at was using a very low dropout voltage regulator, such as TI's LM3940 5V to 3.3V voltage regulator [22].

The second improvement is at the software side. The EP was sending data out every 5 seconds, meaning it goes to sleep for 5 seconds and wakes up for measurements. The reason being for 5 seconds was because during that 5 seconds sleep time, the MSP430 consume the least amount of power. If we were to extend the sleep time to a longer period, we could save and reserve even more energy in our super capacitor. For example, a 30 minutes sleep time. The EP would sends out measurement data every 30 minutes and goes back to sleep. However, there's a limitation to such improvement, as the 16-bit timer can only generate a 5 seconds real-time clock for us at the current operating frequency. A longer real-time clock means it would need to operate at an even lower frequency or having multiple timer interrupts that allows the MSP430 to sleep and wake up multiple times before taking measurements. This is something we will look into to create an applicable application.

The third improvement is at the interface and display software. The current display software can only support up to 1 EP. Multiple EP will be required for a real-world application. More interface options are needed to implement in the software. An ideal interface option was to be able click on a button to initiate a radio-wakeup for the CC2500, so that we could control the EP to take measurement when needed and goes back to sleep when not needed.

Overall, the application fulfills the requirement for being low power application for our harvesting project. It solved the power consumption problem and able to sends important data back to the host. Improvements on this application will be looked at to make this application robust and applicable for real-world scenario.

5.8. Codes

Program codes for the wireless kit and the display program will be provided at the index page. Notice that the codes for the kit has multiple components and libraries for vary parts, including the CC2500 and simpliciTI. A complete set of code can be found at http://www.ti.com/tool/ez430-rf2500 However; it needs to combine with the AP and EP codes

below to make the kit operate as what we had. The AP code below changes the analog-to-digital converter calibration to better match the temperature reading. The EP code below changes the sleep time to 5 seconds versus 1 second.

The code for the interface and display required the program “Processing” to run. Also a UC banner background is required in the directory folder.

6. BIOGRAPHY

[1] AM Query -- AM Radio Technical Information -- Audio Division (FCC) USA. Available: http://transition.fcc.gov/mb/audio/amq.html

[2] FM Query -- FM Radio Technical Information -- Audio Division (FCC) USA. Available: http://transition.fcc.gov/mb/audio/fmq.html

[3] TV Query - TV Technical Information - Video Division - MB (FCC). Available: http://transition.fcc.gov/fcc-bin/audio/tvq.html

[4] AntennaSearch - Search for Cell Towers, Cell Reception, Hidden Antennas and more. Available: http://www.antennasearch.com/

[5] T. Paing, J. Shin, R. Zane, and Z. Popovic, "Resistor emulation approach to low-power RF energy harvesting," Ieee Transactions on Power Electronics, vol. 23, pp. 1494-1501, May 2008.

[6] L. Albasha, S. Heydari Nasab, M. Asefi, and N. Qaddoumi, "Investigation of RF signal energy harvesting," Active and Passive Electronic Components, vol. 2010, 2010.

[7] H. Jabbar, Y. S. Song, and T. T. Jeong, "RF Energy Harvesting System and Circuits for Charging of Mobile Devices," Ieee Transactions on Consumer Electronics, vol. 56, pp. 247-253, Feb 2010.

[8] T. Paing, E. Falkenstein, R. Zane, and Z. Popovic, "Custom IC for ultra-low power RF energy harvesting," in 24th Annual IEEE Applied Power Electronics Conference and Exposition, APEC 2009, February 15, 2009 - February 19, 2009, Washington, DC, United states, 2009, pp. 1239-1245.

[9] D. W. Harrist, "Wireless battery charging system using radio frequency energy harvesting," University of Pittsburgh, 2004.

[10] J. 0. Everly, Back to the Future – Another look at the Crystal Radio, Four Days in May 2011, Fairborn, Ohio

[11] C. Adams, Manhattan Building Techniques, http://www.k7qo.net/manart.pdf.

[12] “Capcitor.” Wikipedia. Web. 10 April 2012. <http://en.wikipedia.org/wiki/Capacitor>

[13] “Electric double-layer capacitor.” Wikipedia. Web. 10 April 2012. <http://en.wikipedia.org/wiki/Electric_double-layer_capacitor>

[14] “Lithium-ion battery.” Wikipedia. Web. 10 April 2012. <http://en.wikipedia.org/wiki/Lithium-ion_battery>

[15] Isidor Buchmann. “Supercapacitor.” Battery University. Web. 23 April 2012. <http://batteryuniversity.com/learn/article/whats_the_role_of_the_supercapacitor>

[15] Isidor Buchmann. “Lithium-Based Batteries.” Battery University. Web. 28. May 2012. <http://batteryuniversity.com/learn/article/lithium_based_batteries>

[16] “LTC4425 – Linear SuperCap Charger with Current-Limited Ideal Diode and V/I Monitor.” Linear Technology. Web. 16 May 2012. <http://www.linear.com/product/LTC4425>

[17] “Zener Diode.” Wikipedia. Web. 27 May 2012. <http://en.wikipedia.org/wiki/Zener_diode>

[18] Boylestad. INTRODUCTORY CIRCUIT ANALYSIS.7th Ed. Columbus: PEARSON Prentice Hall, 2007. Pg. 416.

[19] Texas Instruments. “EZ430-RF2500.” Wikiedpia. Web. 25 May 2012. <http://processors.wiki.ti.com/index.php/EZ430-RF2500>

[20] Texas Instruments. “MSP430.” Wikipedia. Web. 21 March 2012. <http://processors.wiki.ti.com/index.php/MSP430>

[20] Texas Instruments. “MSP430 LaunchPad (MSP-EXP430G2).” Wikipedia. Web. 22 March 2012. <http://processors.wiki.ti.com/index.php/MSP430_LaunchPad_(MSP-EXP430G2)>

[20] “MIXED SIGNAL CONTROLLER.” Texas Instruments. Web. 2 May 2012. <http://www.ti.com/lit/ds/slas504f/slas504f.pdf>

[20] “MSP430x2xx Family User’s Guide.” Texas Instruments. Web. 1 March 2012. <http://www.ti.com/lit/ug/slau144i/slau144i.pdf>

[20] John H. Davies. MSP430 Microcontroller Basics. Newnes. 2008.

[21] Ben Fry and Case Reas. “Processing.” Processing. Web. 28 February 2012. http://processing.org/

[22] “LM3940.” Texas Instruments. Web. 4 June 2012. <http://www.ti.com/product/lm3940>

[23] Windestal, David. “A simple explanation of antenna gain.” RCExplorer. N.d. Web. 4 June 2012. <http:// rcexplorer.se/Educational/gain/gain.html>

[24] “Antenna aperture.” Wikipedia. 9 May 2012. Web. 4 June 2012. <http://en.wikipedia.org/wiki/Antenna_ aperture>

[25] “Effective Area (Effective Aperture).” Antenna-Theory.com. 2009 – 2011. Web. 4 June 2012. <http:// www.antenna-theory.com/basics/aperture.php>

[26] “AM Loop Antennas.” EarMark Productions. 2008. Web. 4 June 2012. <http://www.earmark.net/gesr/ loop/>

[27] Dale, James. “Loop Antennas.” Minnesota DX Club. 22 May 2005. Web. 4 June 2012. <http://www. frontiernet.net/~jadale/Loop.htm>

[28] “Q factor.” Wikipedia. 4 June 2012. Web. 4 June 2012. <http://en.wikipedia.org/wiki/Q_factor>

[29] Carr, Joseph, and George Hippisley. Practical Antenna Handbook. 5th Ed. New York: McGraw-Hill Professional, 2011. Print.

7. BIOSKETCHES

Jason Reese is a Senior Electrical Engineering Technology student at the University of Cincinnati. His course work to date includes, but is not limited to, Circuit Analysis, Electronic Communications, Linear Electronics, Embedded Systems, Digital Signal Processing, and Feedback Control. His previous projects include a Bluetooth controlled power supply. Jason is an Engineering co-op employee at Harris Broadcast Communications. At Harris, Jason has had the opportunity to become familiar with high powered RF transmitters, spectrum and network analyzers, and linear amplifier circuits. Jason hopes to pursue a career in RF technology when he graduates from the University of Cincinnati after the spring 2012 quarter.

Kenneth K. Brown is also a Senior Electrical Engineering Technology student at the University of Cincinnati. He has taken 230 credit hours of undergraduate engineering classes, 193 hour being in the BS of EET program at OCAS. Ken is currently a research chemist and team leader at the National Institute for Occupational Safety and Health (NIOSH), and project officer on the Chemical Exposure Monitoring with Indoor Position (CEMWIP). He hopes to graduate the BSEET program in the spring of 2012 and conduct future research using his electrical engineering technology education to develop methods for hazardous exposure assessment using Direct Reading Methods (DRM).

Jian Zhen, senior Electrical Engineering Technology student at the University of Cincinnati, College of Engineering and Applied Science. Completed 2007 curriculum course works with Winter and Spring quarters yet to finish. Course work related projects including Programmable Power Supply, Alarm Clock, and varies embedded controller labs. Jian was also an Engineering Co-op at Harris Broadcast Communications for five quarter terms; dealing with manufacturing automation testing development for varies communication products, as well as power amplifiers. Jian plans to graduate by the end of Spring quarter, 2012.

8. APPENDIX

8.1.Appendix A

ACCESS POINT CODE

```
#include <string.h>
#include "bsp.h"
#include "mrfi.h"
#include "bsp_leds.h"
#include "bsp_buttons.h"
#include "nwk_types.h"
#include "nwk_api.h"
#include "nwk_frame.h"
#include "nwk.h"
#include "virtual_com_cmds.h"

/* Frequency Agility helper functions */
static void    checkChangeChannel(void);
static void    changeChannel(void);

__interrupt void ADC10_ISR(void);
__interrupt void Timer_A (void);

/*------------------------------------------------------------------------------
 * Globals
 *------------------------------------------------------------------------------*/
/* reserve space for the maximum possible peer Link IDs */
static linkID_t sLID[NUM_CONNECTIONS] = {0};
static uint8_t  sNumCurrentPeers = 0;

/* callback handler */
static uint8_t sCB(linkID_t);

/* received message handler */
static void processMessage(linkID_t, uint8_t *, uint8_t);

/* work loop semaphores */
static volatile uint8_t sPeerFrameSem = 0;
static volatile uint8_t sJoinSem = 0;
static volatile uint8_t sSelfMeasureSem = 0;

/* blink LEDs when channel changes... */
```

```
static volatile uint8_t sBlinky = 0;

/* data for terminal output */
const char splash[] = {"\r\n---------------------------------------------------  \r\n     ****\r\n
****         eZ430-RF2500\r\n     ******o****    Temperature Sensor
Network\r\n********_///_****   Copyright 2009\r\n ******/_//_/*****  Texas
Instruments Incorporated\r\n  ** ***(__/*****   All rights reserved.\r\n     *********
SimpliciTI1.1.1\r\n      *****\r\n       ***\r\n---------------------------------------------------
\r\n"};
volatile int * tempOffset = (int *)0x10F4;

/*-------------------------------------------------------------------------
 * Frequency Agility support (interference detection)
 *-------------------------------------------------------------------------*/
#ifdef FREQUENCY_AGILITY

#define INTERFERNCE_THRESHOLD_DBM (-70)
#define SSIZE    25
#define IN_A_ROW  3
static int8_t  sSample[SSIZE];
static uint8_t sChannel = 0;

#endif  /* FREQUENCY_AGILITY */

/*-------------------------------------------------------------------------
 * Main
 *-------------------------------------------------------------------------*/
void main (void)
{
  bspIState_t intState;

#ifdef FREQUENCY_AGILITY
  memset(sSample, 0x0, sizeof(sSample));
#endif

  /* Initialize board */
  BSP_Init();

  /* Initialize TimerA and oscillator */
  BCSCTL3 |= LFXT1S_2;                  // LFXT1 = VLO
  TACCTL0 = CCIE;                      // TACCR0 interrupt enabled
  TACCR0 = 12000;                       // ~1 second
  TACTL = TASSEL_1 + MC_1;              // ACLK, upmode
```

```
/* Initialize serial port */
COM_Init();

//Transmit splash screen and network init notification
TXString( (char*)splash, sizeof splash);
TXString( "\r\nInitializing Network....", 26 );

SMPL_Init(sCB);

// network initialized
TXString( "Done\r\n", 6);

/* green and red LEDs on solid to indicate waiting for a Join. */
BSP_TURN_ON_LED1();
BSP_TURN_ON_LED2();

/* main work loop */
while (1)
{
 /* Wait for the Join semaphore to be set by the receipt of a Join frame from
  * a device that supports an End Device.
  *
  * An external method could be used as well. A button press could be connected
  * to an ISR and the ISR could set a semaphore that is checked by a function
  * call here, or a command shell running in support of a serial connection
  * could set a semaphore that is checked by a function call.
  */
 if (sJoinSem && (sNumCurrentPeers < NUM_CONNECTIONS))
 {
  /* listen for a new connection */
  while (1)
  {
   if (SMPL_SUCCESS == SMPL_LinkListen(&sLID[sNumCurrentPeers]))
   {
    break;
   }
   /* Implement fail-to-link policy here. otherwise, listen again. */
  }

  sNumCurrentPeers++;

  BSP_ENTER_CRITICAL_SECTION(intState);
  sJoinSem--;
  BSP_EXIT_CRITICAL_SECTION(intState);
```

```
}


// if it is time to measure our own temperature...
if(sSelfMeasureSem)
{
  char msg [6];
  char addr[] = {"HUB0"};
  char rssi[] = {"000"};
  int degC, volt;
  volatile long temp;
  int results[2];

  /* Get temperature */
  ADC10CTL1 = INCH_10 + ADC10DIV_4;       // Temp Sensor ADC10CLK/5
  ADC10CTL0 = SREF_1 + ADC10SHT_3 + REFON + ADC10ON + ADC10IE + ADC10SR;
  /* Allow ref voltage to settle for at least 30us (30us * 8MHz = 240 cycles)
   * See SLAS504D for settling time spec
   */
  __delay_cycles(240);
  ADC10CTL0 |= ENC + ADC10SC;             // Sampling and conversion start
  __bis_SR_register(CPUOFF + GIE);        // LPM0 with interrupts enabled
  results[0] = ADC10MEM;                  // Retrieve result
  ADC10CTL0 &= ~ENC;

  /* Get voltage */
  ADC10CTL1 = INCH_11;                     // AVcc/2
  ADC10CTL0 = SREF_1 + ADC10SHT_2 + REFON + ADC10ON + ADC10IE + REF2_5V;
  __delay_cycles(240);
  ADC10CTL0 |= ENC + ADC10SC;             // Sampling and conversion start
  __bis_SR_register(CPUOFF + GIE);        // LPM0 with interrupts enabled
  results[1] = ADC10MEM;                  // Retrieve result

  /* Stop and turn off ADC */
  ADC10CTL0 &= ~ENC;
  ADC10CTL0 &= ~(REFON + ADC10ON);


     temp = ADC10MEM;


  /* oC = ((A10/1024)*1500mV)-986mV)*1/3.55mV = A10*423/1024 - 278
   * the temperature is transmitted as an integer where 32.1 = 321
   * hence 4230 instead of 423
```

```
  */
  temp = results[0];
  //degC = ((temp - 673) * 4230) / 1024;
  degC = ((temp - 691) * 4230) / 1024;
  if( (*tempOffset) != 0xFFFF )
  {
    degC += (*tempOffset);
  }

  temp = results[1];
  volt = (temp*25)/512;

  /* Package up the data */
  msg[0] = degC&0xFF;
  msg[1] = (degC>>8)&0xFF;
  msg[2] = volt;

  /* Send it over serial port */
  transmitDataString(1, addr, rssi, msg );

  BSP_TOGGLE_LED1();

  /* Done with measurement, disable measure flag */
  sSelfMeasureSem = 0;
}

/* Have we received a frame on one of the ED connections?
 * No critical section -- it doesn't really matter much if we miss a poll
 */
if (sPeerFrameSem)
{
  uint8_t     msg[MAX_APP_PAYLOAD], len, i;

  /* process all frames waiting */
  for (i=0; i<sNumCurrentPeers; ++i)
  {
    if (SMPL_SUCCESS == SMPL_Receive(sLID[i], msg, &len))
    {
      ioctlRadioSiginfo_t sigInfo;

      processMessage(sLID[i], msg, len);

      sigInfo.lid = sLID[i];
```

```
        SMPL_Ioctl(IOCTL_OBJ_RADIO, IOCTL_ACT_RADIO_SIGINFO, (void *)&sigInfo);

        transmitData( i, sigInfo.sigInfo.rssi, (char*)msg );
        BSP_TOGGLE_LED2();

        BSP_ENTER_CRITICAL_SECTION(intState);
        sPeerFrameSem--;
        BSP_EXIT_CRITICAL_SECTION(intState);
       }
     }
    }
    if (BSP_BUTTON1())
    {
     __delay_cycles(2000000);  /* debounce (0.25 seconds) */
     changeChannel();
    }
    else
    {
     checkChangeChannel();
    }
    BSP_ENTER_CRITICAL_SECTION(intState);
    if (sBlinky)
    {
     if (++sBlinky >= 0xF)
     {
      sBlinky = 1;
      BSP_TOGGLE_LED1();
      BSP_TOGGLE_LED2();
     }
    }
    BSP_EXIT_CRITICAL_SECTION(intState);
  }

}

/* Runs in ISR context. Reading the frame should be done in the */
/* application thread not in the ISR thread. */
static uint8_t sCB(linkID_t lid)
{
  if (lid)
  {
    sPeerFrameSem++;
    sBlinky = 0;
  }
```

```
  else
  {
    sJoinSem++;
  }

  /* leave frame to be read by application. */
  return 0;
}

static void processMessage(linkID_t lid, uint8_t *msg, uint8_t len)
{
  /* do something useful */
  if (len)
  {
    BSP_TOGGLE_LED1();
  }
  return;
}

static void changeChannel(void)
{
#ifdef FREQUENCY_AGILITY
  freqEntry_t freq;

  if (++sChannel >= NWK_FREQ_TBL_SIZE)
  {
    sChannel = 0;
  }
  freq.logicalChan = sChannel;
  SMPL_Ioctl(IOCTL_OBJ_FREQ, IOCTL_ACT_SET, &freq);
  BSP_TURN_OFF_LED1();
  BSP_TURN_OFF_LED2();
  sBlinky = 1;
#endif
  return;
}

/* implement auto-channel-change policy here... */
static void checkChangeChannel(void)
{
#ifdef FREQUENCY_AGILITY
  int8_t dbm, inARow = 0;

  uint8_t i;
```

```
  memset(sSample, 0x0, SSIZE);
  for (i=0; i<SSIZE; ++i)
  {
    /* quit if we need to service an app frame */
    if (sPeerFrameSem || sJoinSem)
    {
      return;
    }
    NWK_DELAY(1);
    SMPL_Ioctl(IOCTL_OBJ_RADIO, IOCTL_ACT_RADIO_RSSI, (void *)&dbm);
    sSample[i] = dbm;

    if (dbm > INTERFERNCE_THRESHOLD_DBM)
    {
      if (++inARow == IN_A_ROW)
      {
        changeChannel();
        break;
      }
    }
    else
    {
      inARow = 0;
    }
  }
#endif
  return;
}

/*-------------------------------------------------------------------------
* ADC10 interrupt service routine
-------------------------------------------------------------------------*/
#pragma vector=ADC10_VECTOR
__interrupt void ADC10_ISR(void)
{
  __bic_SR_register_on_exit(CPUOFF);        // Clear CPUOFF bit from 0(SR)
}

/*-------------------------------------------------------------------------
* Timer A0 interrupt service routine
-------------------------------------------------------------------------*/
#pragma vector=TIMERA0_VECTOR
__interrupt void Timer_A (void)
```

```
{
  sSelfMeasureSem = 1;
}
```

END POINT CODE

```
#include "bsp.h"
#include "mrfi.h"
#include "nwk_types.h"
#include "nwk_api.h"
#include "bsp_leds.h"
#include "bsp_buttons.h"
#include "vlo_rand.h"

/*------------------------------------------------------------------------------
 * Defines
 *------------------------------------------------------------------------------*/
/* How many times to try a TX and miss an acknowledge before doing a scan */
#define MISSES_IN_A_ROW  2

/*------------------------------------------------------------------------------
 * Prototypes
 *------------------------------------------------------------------------------*/
static void linkTo(void);
void createRandomAddress(void);
__interrupt void ADC10_ISR(void);
__interrupt void Timer_A (void);

/*------------------------------------------------------------------------------
* Globals
------------------------------------------------------------------------------*/
static linkID_t sLinkID1 = 0;
/* Temperature offset set at production */
volatile int * tempOffset = (int *)0x10F4;
/* Initialize radio address location */
char * Flash_Addr = (char *)0x10F0;
/* Work loop semaphores */
static volatile uint8_t sSelfMeasureSem = 0;

/*------------------------------------------------------------------------------
 * Main
 *------------------------------------------------------------------------------*/
void main (void)
{
  addr_t lAddr;

  /* Initialize board-specific hardware */
  BSP_Init();
```

```
/* Check flash for previously stored address */
if(Flash_Addr[0] == 0xFF && Flash_Addr[1] == 0xFF &&
   Flash_Addr[2] == 0xFF && Flash_Addr[3] == 0xFF )
{
  createRandomAddress(); // Create and store a new random address
}

/* Read out address from flash */
lAddr.addr[0] = Flash_Addr[0];
lAddr.addr[1] = Flash_Addr[1];
lAddr.addr[2] = Flash_Addr[2];
lAddr.addr[3] = Flash_Addr[3];

/* Tell network stack the device address */
SMPL_Ioctl(IOCTL_OBJ_ADDR, IOCTL_ACT_SET, &lAddr);

/* Initialize TimerA and oscillator */
BCSCTL3 |= LFXT1S_2;                  // LFXT1 = VLO
TACCTL0 = CCIE;                      // TACCR0 interrupt enabled
TACCR0 = 12000;                       // ~ 1 sec
TACTL = TASSEL_1 + MC_2;              // ACLK, upmode

/* Keep trying to join (a side effect of successful initialization) until
 * successful. Toggle LEDS to indicate that joining has not occurred.
 */
while (SMPL_SUCCESS != SMPL_Init(0))
{
  BSP_TOGGLE_LED1();
  BSP_TOGGLE_LED2();
  /* Go to sleep (LPM3 with interrupts enabled)
   * Timer A0 interrupt will wake CPU up every second to retry initializing
   */
  __bis_SR_register(LPM3_bits+GIE);  // LPM3 with interrupts enabled
}

/* LEDs on solid to indicate successful join. */
BSP_TURN_ON_LED1();
BSP_TURN_ON_LED2();

/* Unconditional link to AP which is listening due to successful join. */
linkTo();

while(1);
```

```
}

static void linkTo()
{
  uint8_t msg[3];
#ifdef APP_AUTO_ACK
  uint8_t misses, done;
#endif

  /* Keep trying to link... */
  while (SMPL_SUCCESS != SMPL_Link(&sLinkID1))
  {
    BSP_TOGGLE_LED1();
    BSP_TOGGLE_LED2();
    /* Go to sleep (LPM3 with interrupts enabled)
     * Timer A0 interrupt will wake CPU up every second to retry linking
     */
    __bis_SR_register(LPM3_bits+GIE);
  }

  /* Turn off LEDs. */
  BSP_TURN_OFF_LED1();
  BSP_TURN_OFF_LED2();

  /* Put the radio to sleep */
  SMPL_Ioctl(IOCTL_OBJ_RADIO, IOCTL_ACT_RADIO_SLEEP, 0);

  while (1)
  {
    /* Go to sleep, waiting for interrupt every second to acquire data */
    __bis_SR_register(LPM3_bits);

    /* Time to measure */
    if (sSelfMeasureSem) {
      volatile long temp;
      int degC, volt;
      int results[2];
#ifdef APP_AUTO_ACK
      uint8_t     noAck;
      smplStatus_t rc;
#endif

      /* Get temperature */
```

```
    ADC10CTL1 = INCH_10 + ADC10SSEL_1;// + ADC10DIV_4;       // Temp Sensor
ADC10CLK/5
    ADC10CTL0 = SREF_1 + ADC10SHT_3 + REFON + ADC10ON + ADC10IE + ADC10SR;
    /* Allow ref voltage to settle for at least 30us (30us * 8MHz = 240 cycles)
     * See SLAS504D for settling time spec
     */
    //__delay_cycles(240);
    ADC10CTL0 |= ENC + ADC10SC;             // Sampling and conversion start
    __bis_SR_register(CPUOFF + GIE);        // LPM0 with interrupts enabled
    results[0] = ADC10MEM;                  // Retrieve result
    ADC10CTL0 &= ~ENC;

    /* Get voltage */
    ADC10CTL1 = INCH_11 + ADC10SSEL_1;                  // AVcc/2
    ADC10CTL0 = SREF_1 + ADC10SHT_2 + REFON + ADC10ON + ADC10IE + REF2_5V;
   // __delay_cycles(240);
    ADC10CTL0 |= ENC + ADC10SC;             // Sampling and conversion start
    __bis_SR_register(CPUOFF + GIE);        // LPM0 with interrupts enabled
    results[1] = ADC10MEM;                  // Retrieve result

    /* Stop and turn off ADC */
    ADC10CTL0 &= ~ENC;
    ADC10CTL0 &= ~(REFON + ADC10ON);

    /* oC = ((A10/1024)*1500mV)-986mV)*1/3.55mV = A10*423/1024 - 278
     * the temperature is transmitted as an integer where 32.1 = 321
     * hence 4230 instead of 423
     */
    temp = results[0];
    degC = ((temp - 672) * 4230) / 1024;
    if( (*tempOffset) != 0xFFFF )
    {
      degC += (*tempOffset);
    }

    /* message format,  UB = upper Byte, LB = lower Byte
    -------------------------------
    |degC LB | degC UB |  volt LB |
    -------------------------------
      0       1        2
    */
    temp = results[1];
    volt = (temp*25)/512;
    msg[0] = degC&0xFF;
```

```
    msg[1] = (degC>>8)&0xFF;
    msg[2] = volt;

    /* Get radio ready...awakens in idle state */
    SMPL_Ioctl( IOCTL_OBJ_RADIO, IOCTL_ACT_RADIO_AWAKE, 0);

#ifdef APP_AUTO_ACK
    /* Request that the AP sends an ACK back to confirm data transmission
     * Note: Enabling this section more than DOUBLES the current consumption
     *       due to the amount of time IN RX waiting for the AP to respond
     */
    done = 0;
    while (!done)
    {
      noAck = 0;

      /* Try sending message MISSES_IN_A_ROW times looking for ack */
      for (misses=0; misses < MISSES_IN_A_ROW; ++misses)
      {
        if (SMPL_SUCCESS == (rc=SMPL_SendOpt(sLinkID1, msg, sizeof(msg),
SMPL_TXOPTION_ACKREQ)))
        {
          /* Message acked. We're done. Toggle LED 1 to indicate ack received. */
          BSP_TURN_ON_LED1();
          __delay_cycles(2000);
          BSP_TURN_OFF_LED1();
          break;
        }
        if (SMPL_NO_ACK == rc)
        {
          /* Count ack failures. Could also fail becuase of CCA and
           * we don't want to scan in this case.
           */
          noAck++;
        }
      }
      if (MISSES_IN_A_ROW == noAck)
      {
        /* Message not acked */
        BSP_TURN_ON_LED2();
        __delay_cycles(2000);
        BSP_TURN_OFF_LED2();
#ifdef FREQUENCY_AGILITY
        /* Assume we're on the wrong channel so look for channel by
```

```
         * using the Ping to initiate a scan when it gets no reply. With
         * a successful ping try sending the message again. Otherwise,
         * for any error we get we will wait until the next button
         * press to try again.
         */
        if (SMPL_SUCCESS != SMPL_Ping(sLinkID1))
        {
          done = 1;
        }
#else
        done = 1;
#endif  /* FREQUENCY_AGILITY */
      }
      else
      {
        /* Got the ack or we don't care. We're done. */
        done = 1;
      }
    }
#else

    /* No AP acknowledgement, just send a single message to the AP */
    SMPL_SendOpt(sLinkID1, msg, sizeof(msg), SMPL_TXOPTION_NONE);

#endif /* APP_AUTO_ACK */

    /* Put radio back to sleep */
    SMPL_Ioctl( IOCTL_OBJ_RADIO, IOCTL_ACT_RADIO_SLEEP, 0);

    /* Done with measurement, disable measure flag */
    sSelfMeasureSem = 0;
  }
 }
}

void createRandomAddress()
{
 unsigned int rand, rand2;
 do
 {
  rand = TI_getRandomIntegerFromVLO();    // first byte can not be 0x00 of 0xFF
 }
 while( (rand & 0xFF00)==0xFF00 || (rand & 0xFF00)==0x0000 );
 rand2 = TI_getRandomIntegerFromVLO();
```

```
  BCSCTL1 = CALBC1_1MHZ;                // Set DCO to 1MHz
  DCOCTL = CALDCO_1MHZ;
  FCTL2 = FWKEY + FSSEL0 + FN1;          // MCLK/3 for Flash Timing Generator
  FCTL3 = FWKEY + LOCKA;                // Clear LOCK & LOCKA bits
  FCTL1 = FWKEY + WRT;                  // Set WRT bit for write operation

  Flash_Addr[0]=(rand>>8) & 0xFF;
  Flash_Addr[1]=rand & 0xFF;
  Flash_Addr[2]=(rand2>>8) & 0xFF;
  Flash_Addr[3]=rand2 & 0xFF;

  FCTL1 = FWKEY;                        // Clear WRT bit
  FCTL3 = FWKEY + LOCKA + LOCK;         // Set LOCK & LOCKA bit
}

/*-------------------------------------------------------------------------
 * ADC10 interrupt service routine
 *-------------------------------------------------------------------------*/
#pragma vector=ADC10_VECTOR
__interrupt void ADC10_ISR(void)
{
  __bic_SR_register_on_exit(CPUOFF);       // Clear CPUOFF bit from 0(SR)
}

/*-------------------------------------------------------------------------
 * Timer A0 interrupt service routine
 *-------------------------------------------------------------------------*/
#pragma vector=TIMERA0_VECTOR
__interrupt void Timer_A (void)
{
  sSelfMeasureSem = 1;
  __bic_SR_register_on_exit(LPM3_bits);       // Clear LPM3 bit from 0(SR)
}
```

Interface and Display Codes

```
import controlP5.*;
import de.looksgood.ani.*;
import de.looksgood.ani.easing.*;
PFont Menufont;
int i, COMPort, dataRead, keyIndex=10,welcome=1, key1=1, onlineyr, onlinemon,
onlineday, onlinehr, onlinemin, onlinesec;
float APtemp, ED1temp, ED1signal, ED2temp, ED2signal;
float lowAPtemp = 999, highAPtemp = 0, lowED1temp = 999, highED1temp = 0,
lowED2temp = 999, highED2temp = 0;
String APlowtemp, APcurrenttemp, APhightemp, APvolt, ED1lowtemp, ED1currenttemp,
ED1hightemp, ED1volt, ED1yr, ED1mon, ED1day, ED1hr, ED2lowtemp, ED2currenttemp,
ED2hightemp, ED2volt, ED2yr, ED2mon, ED2day, ED2hr, ED2min, ED2sec;
int [] keyIn = new int[11];
boolean portChosen = false;
Serial myPort;
PImage banner;
void setup()
{ // Start of Setup
// Banner & Background
background(0);
size(900, 500);
banner = loadImage("UCBanner.jpg");
image(banner,0,0);
// Welcome text
if(welcome == 1){
Menufont = loadFont("ComicSansMS-12.vlw");
textFont(Menufont, 25);
text("WELCOME TO THE RF HARVESTING PROJECT", 160, 250);
textSize(15);
text("Press Enter To Start The Application", 320, 300);
} // End of Welcome text
} // End of Setup
void keyPressed()
{ // Start of Key Pressed function
 if (key1 == 1 & key == ENTER) // Start of ENTER key pressed
{
welcome = 0; // Disable welcome text
key1 = 0; // Disable ENTER key
setup(); // Call setup for screen
// Check and list COM ports
import processing.serial.*;
for(i=0;i<Serial.list().length;i++)
{
```

```
 //text("["+i+"] " + Serial.list()[i],10, 140+14*i);
  }
 }

 if(portChosen == false & key1 == 0){

     while(i<10)
     {
      myPort = new Serial(this, Serial.list()[i-1],9600); //2400 for msp430 only
     dataRead = myPort.read();

    if(dataRead != -1 || dataRead == -1)
   {
     portChosen = true;
     text("Please press the MSP430 start button to start temperature reading", 10, 120);
     break;
   }
   else {
    i = i - 1;
   }
     }
 }

} // End of Key Pressed function

void draw()
{ // Begin of Draw

 if(portChosen == true)
  {
   dataRead = myPort.read();
  if(dataRead != -1 & dataRead !=248)
  {

    background(0);
    size(900, 500);
    image(banner,0,0);

    delay(1000);
    String inBuffer = myPort.readString();
    int leng = inBuffer.length();
    if (inBuffer != null && leng > 40) { // begin serial data reading
    String Datastring = inBuffer;
  //  println(Datastring);
```

```
 //Node 0 (AP) readings
 if(Datastring.substring(1, 16).equals("Node:HUB0,Temp:") == true) {
 APtemp = float(Datastring.substring(17, 21));
 println("AP temp:" + APtemp);
 APvolt = Datastring.substring(31, 34);
 println("AP Volt:" + APvolt);
 } // End of Node 0 reading
   //Node 1 (ED) readings
 else if(Datastring.substring(1, 6).equals("$0001") == true) {
  ED1temp = float(Datastring.substring(8, 12));
  println("ED1 temp:" + ED1temp);
  ED1volt = Datastring.substring(14, 17);
  println("ED1 volt:" + ED1volt);
  ED1signal = float(Datastring.substring(18, 21));
  println("ED1 signal:" + ED1signal);
onlineyr = year();
 ED1yr = String.valueOf(onlineyr);
 onlinemon = month();
 ED1mon = String.valueOf(onlinemon);
 onlineday = day();
 ED1day = String.valueOf(onlineday);
 onlinehr = hour();
 ED1hr = String.valueOf(onlinehr);
 onlinemin = minute();
 onlinesec = second();
 } // End of Node 1 readings
  //Node 2 (ED) readings
 else if(Datastring.substring(1, 6).equals("$0002") == true) {
  ED1temp = float(Datastring.substring(8, 12));
  println("ED2 temp:" + ED2temp);
  ED1volt = Datastring.substring(14, 17);
  println("ED2 volt:" + ED2volt);
  ED1signal = float(Datastring.substring(18, 21));
  println("ED2 signal:" + ED2signal);
 onlineyr = year();
 ED2yr = String.valueOf(onlineyr);
 onlinemon = month();
 ED2mon = String.valueOf(onlinemon);
 onlineday = day();
 ED2day = String.valueOf(onlineday);
 onlinehr = hour();
 ED2hr = String.valueOf(onlinehr);
 onlinemin = minute();
 onlinesec = second();
```

```
   } // End of Node 2 readings
  } // End of Data reading from serial port
displayAPtemp(); // AP temperature
if(ED1volt != null){
 displayED1();
 }
 if(ED2volt != null){
  displayED2();
 }
    }  // End of if dataRead
  } // End of port chosen
} // End of Draw
void displayAPtemp() //AP temperature reading on GUI function
{
     if(lowAPtemp >= APtemp) // Calculate Lowest Temp
     {
       lowAPtemp = APtemp;
       APlowtemp = nf(lowAPtemp,1,1);
     }

     if(highAPtemp <= APtemp) // Calculate Highest Temp
     {
       highAPtemp = APtemp;
       APhightemp = nf(highAPtemp,1,1);
     }

     APcurrenttemp = nf(APtemp,1,1); // Current Temp
     text("Access Point Lowest  Temperature: ", 10, 120);
     text(APlowtemp, 255, 120);
     text("°F", 285, 120);
     text("Access Point Current Temperature: ", 10, 135);
     text(APcurrenttemp, 255, 135);
     text("°F", 285, 135);
     text("Access Point Highest Temperature: ", 10, 150);
     text(APhightemp, 255, 150);
     text("°F", 285, 150);
      text("Access Point Supply Voltage:", 10, 165);
     text(APvolt, 215, 165);
     text("V", 245, 165);
} // End of AP tempeature on GUI function
void displayED1() //ED1 display function
{
     if(lowED1temp >= ED1temp) // Calculate Lowest Temp
     {
```

```
      lowED1temp = ED1temp;
      ED1lowtemp = nf(lowED1temp,1,1);
    }

    if(highED1temp <= ED1temp) // Calculate Highest Temp
    {
      highED1temp = ED1temp;
      ED1hightemp = nf(highED1temp,1,1);
    }
    ED1currenttemp = nf(ED1temp,1,1); // Current Temp
    text("End Point Lowest  Temperature: ", 10, 220);
    text(ED1lowtemp, 235, 220);
    text("°F", 265, 220);

    text("End Point Current Temperature: ", 10, 235);
    text(ED1currenttemp, 235, 235);
    text("°F", 265, 235);

    text("End Point Highest Temperature: ", 10, 250);
    text(ED1hightemp, 235, 250);
    text("°F", 265, 250);

    text("End Point Supply Voltage:", 10, 265);
    text(ED1volt, 195, 265);
    text("V", 225, 265);
    text("Last Reading Was Taken At:" +" "+ onlinemon + "/" + onlineday + "/" + onlineyr
+ ", " + onlinehr + ":" + onlinemin + ":" + onlinesec, 10, 200);

} // End of ED1 display function

void displayED2() //ED2 display function
{

    if(lowED2temp >= ED2temp) // Calculate Lowest Temp
    {
      lowED2temp = ED2temp;
      ED2lowtemp = nf(lowED2temp,1,1);
    }

    if(highED2temp <= ED2temp) // Calculate Highest Temp
    {
      highED2temp = ED2temp;
      ED2hightemp = nf(highED2temp,1,1);
    }
```

```
    ED2currenttemp = nf(ED2temp,1,1); // Current Temp

    text("End Point 2 Lowest  Temperature: ", 10, 320);
    text(ED2lowtemp, 235, 320);
    text("°F", 265, 320);

    text("End Point 2 Current Temperature: ", 10, 335);
    text(ED2currenttemp, 235, 335);
    text("°F", 265, 335);

    text("End Point 2 Highest Temperature: ", 10, 350);
    text(ED2hightemp, 235, 350);
    text("°F", 265, 350);

    text("End Point 2 Supply Voltage:", 10, 365);
    text(ED2volt, 195, 365);
    text("V", 225, 365);
    text("Last Reading Was Taken At:" +" "+ ED2mon + "/" + ED2day + "/" + ED2yr + ", " +
ED2hr + ":" + onlinemin + ":" + onlinesec, 10, 300);

} // End of ED2 display function
```